Development of an end to end spectral image simulator for WEAVE

Sun Jeong Ham

Wolfson College, University of Oxford

Hilary Term 2016

Astrophysics sub-department, Department of Physics, University of Oxford,

Keble Road, Oxford, OX1 3RH, United Kingdom

ABSTRACT

The WHT Extreme Aperture Velocity Explorer (WEAVE) is a form of ground-based wide-field spectrograph, planned to be installed at the prime focus of the 4.2m William Herschel Telescope (WHT). The instrument has a two degree field of view and full coverage of the visible wavelength from 366nm to 950nm. Using fibre-optic pick-offs at the focal plane, it can also observe up to 960 simultaneous spectra for each configuration. The fibre-fed spectrograph consists of a collimator mirror, dichroic and two correcting lenses before each of two volume phase holographic (VPH) gratings and two eight-lens cameras. The two cameras have been designed to have the same lens shapes and have almost the same glass blank and the design also reduces the ghost between the surfaces of the lenses. The unique part of the instrument is called the ‘Positioner’; fibres on the positioner can be moved in the focal plane to pick the required target.

The WEAVE survey is expected to start observing by 2018. Here we report on the development of the details of an end-to-end image simulator for WEAVE which can be used to generate data to test the image processing and analysis pipelines. The WEAVE simulator is aimed to: 1) verify the whole data acquisition, reduction and calibration procedure throughout the WEAVE science processing and archiving (SPA), 2) generate high signal-noise reference images that can be used as fitting templates for the extraction of the real spectra, and Point Spread Function (PSF) mapping and 3) verify the feasibility of the scientific objectives, to allow the survey planning to be optimized before the instrument is commissioned.

Contents

Chapter 1
Introduction

1.1 WEAVE project overview

1.1.1 Scientific objectives

WEAVE [Balcells et al., 2010; Dalton et al., 2012] is new multi-fibre spectrograph facility that is scheduled to be installed at the prime focus of WHT (William Herschel Telescope) at the Roque de los Muchachos observatory, La Palma in the Canary Islands. The first light at the telescope is expected in 2018 and it will operate for at least 5 years until 2023.

The scientific objectives of WEAVE are broadly related to studying galaxy structure and cosmology, the methods and research are linked with ESA's Gaia satellite which launched on 19 December 2012 for a galactic survey and the European Low Frequency Array (LOFAR) for extra-galactic research. WEAVE will provide spectroscopic data to support the Gaia astrometric catalogue and also follow up LOFAR wide-field surveys.

WEAVE's principle scientific objectives focus on three areas- Galactic Archeology, Galaxy Evolution and Cosmology [Dalton et al., 2012; Trager, 2015].

1. Milky Way archaeology: exploiting Gaia's scientific legacy.

   The Gaia satellite was launched to measure the 3D positions and proper motions of more than 10^9 stars in our Galaxy and to study the photometry, stellar parameters and radial velocities of the brightest stars (V<~15), as well as the ages and chemical abundance of the stars in the Milky Way. A goal of this study is also to establish a comprehensive Milky Way spectroscopic census. The WEAVE will provide key data with a high-resolution and low-resolution survey of the fainter stars that Gaia cannot reach spectroscopically.

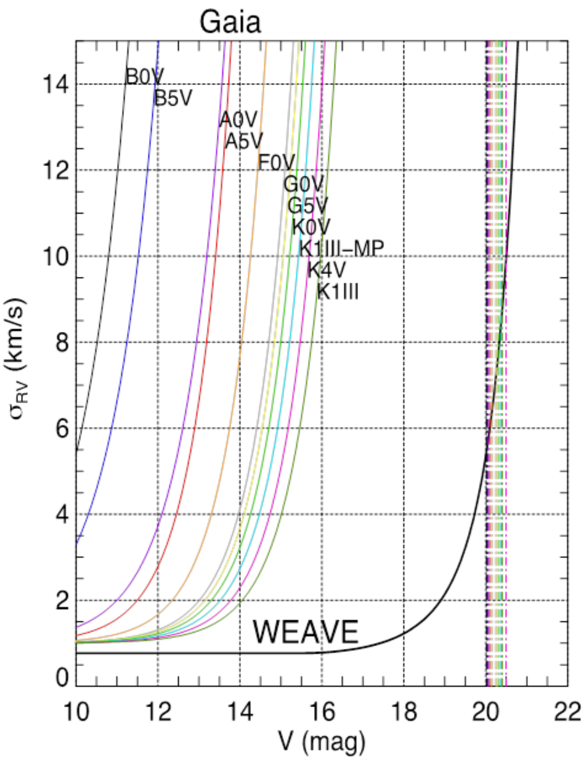

Figure 1 The solid black line represents the predicted radial velocity accuracies for WEAVE at a low resolution, ~ R=5000. The other lines from Gaia, represent the different types of star and their radial velocity limits,which are observable using Gaia, the dashed coloured lines across WEAVE's radial velocity show Gaia's photometric limits for each type at the end of the mission [Trager S. C., 2015].

The WEAVE Milky Way surveys will contain several ranges of targets for the different resolutions, i.e. the low and high resolution of the WEAVE optical system as below.

- The Halo LR survey: The galactic stars which will not be observed spectroscopically by Gaia. WEAVE will target stars located at high galactic latitude (~10,000 deg^2) with V magnitude between 15 and 20. These objectives are expected to provide the information about the Galactic halo such as mass, distance, velocity and formation that cannot reach by previously planned low-resolution spectrographs.
- The Disc Dynamics LR survey: This is for targets lying on low latitudes at the Galactic disc. WEAVE will survey the disc dynamics for ~10^6 targets having a V magnitude between 16 and 20.
- The HR chemo-dynamical survey: This is a high resolution survey for targets at intermediate and high galactic latitudes, with a V magnitude between 12 and 16. In terms of the study for chemo-dynamics, WEAVE will survey three different populations of the Galaxy: the stars in thin and thick discs and also the halo stars.
- The open clusters survey: This is for gathering the information about stellar evolution: a high resolution survey will perform the observations of both old Open Clusters and young clusters in the Galactic disk.

2. Galaxy evolution and cosmology: exploiting the LOFAR and APERTIF surveys.

   APERTIF is the first radio frequency focal plane array that is now installed at the Westerbork telescope. [Verheijen et al., 2008] This project will deliver unique information about the neutral gas distribution from measurements of the HI (21cm) line in 10^4 galaxies. The WEAVE survey will follow the APERTIF medium-deep survey to sample the stellar kinematics and ionized gas in the galaxies in the low redshift survey, it is expected to contain information about the gas and dark matter within the galaxies and to address questions of galaxy evolution and star formation. The WEAVE-LOFAR survey will aim to obtain spectra of around ~ 4×10^6 radio sources; this survey will provide the key information to find out cosmic history from the re-ionisation era and evolution involving the interaction between AGN activity and star-formation [Smith et al., 2015].

1.1.2 Instrument design and structure

The original WEAVE design concept derives from the 2dF instrument for the Anglo-Australia Telescope [Dalton et al., 2012] and the OPTIMOS-EVE spectrograph design study for the E-ELT [Navarro et al., 2010; Chemla et al., 2010]. The system design has been optimised for the WHT facility and its scientific requirements; the overall WEAVE parameters and characteristics are shown in Table 1 and the WHT facility in Figure 2 as below [Trager et al., 2015].

Table 1 The characteristics of WEAVE as determined from the scientific requirements

Specification	Requirement
Field of view diameter	2 deg
MOS multiplex, Plate A/B	960/940
Atmospheric dispersion compensation	0.36-0.95μm, 60ºZD
MOS fibre aperture	≥1.3”
Open shutter efficiency (1hour observations)	70%
Wavelength coverage	366-959nm
Spectral resolution (full simultaneous coverage)	5000
Spectral resolution (reduced coverage)	20000
Stray light as function of faintest target	<1%
Blue system efficiency	20%
Red system efficiency	25%
Multi-IFU multiplex	20
Multi-IFU FOV	10”x 12”
Multi-IFU spaxel size	1.3”
Single IFU FOV	1.3’x 1.5’
Single IFU spaxel size	2.6”

The wavelength coverage is the full visible spectrum from 0.366 to 0.959μm and the required spectral resolution coverage is up to ~7500 for the low resolution mode. The wavelength range for the high resolution mode is 0.404~ 0.406, 0.473~0.545, 0.595~0.685μm and the resolution is up to ~24000.

Figure 2 The WHT in the dome. The WEAVE fibre positioner and prime focus corrector will be located at the prime focus of the telescope. The two Nasmyth enclosures, GRACE (left) and GHRIL (right) are shown in the picture. The WEAVE spectrograph will be located within GHRIL.

The unique part of the instrument is the fibre positioner, which can position the fibres to the required targets using a pick-and-place robot as shown in Figures 3 and 4. It is an important element of the WEAVE system and makes the facility able to observe multiple targets at the same time and for efficient observations of large numbers of targets.

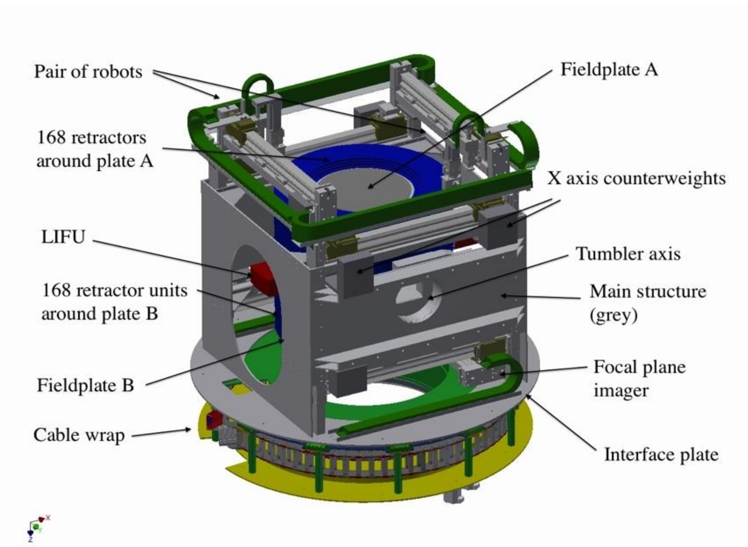

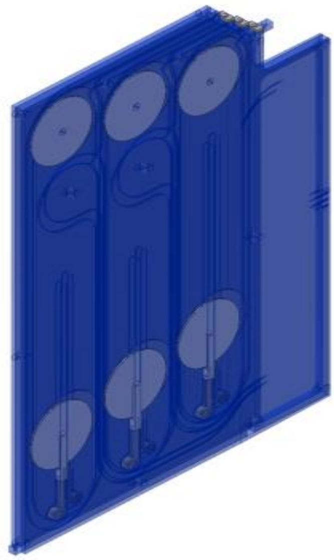

Figure 3 Complete structure design model of the positioner with two positioner robots (left) and the specific part of the fibre retractor unit (right) in the positioner [Dalton et al., 2014] The positioner will be installed at the current flip-ring of the second mirror of WHT as shown in Figure 2.

This positioner concept was adapted from the 2dF instrument in the Anglo Australian Telescope [Lewis et al., 2002]. It has been designed to increase multiplex and efficiency and reduce technical downtime risk during operations with off-the-shelf components and two robots working in parallel.

The graphic of the fibres when positioned on a typical field in the focal plane is represented in Figure 4 as below. The fibre bundle is divided at the positioner, as shown in Figure 5. In the MOS mode, there are 24 fibres in one slitlet, and 40 slitlets are arranged in the slit, which has 960 fibres in total.

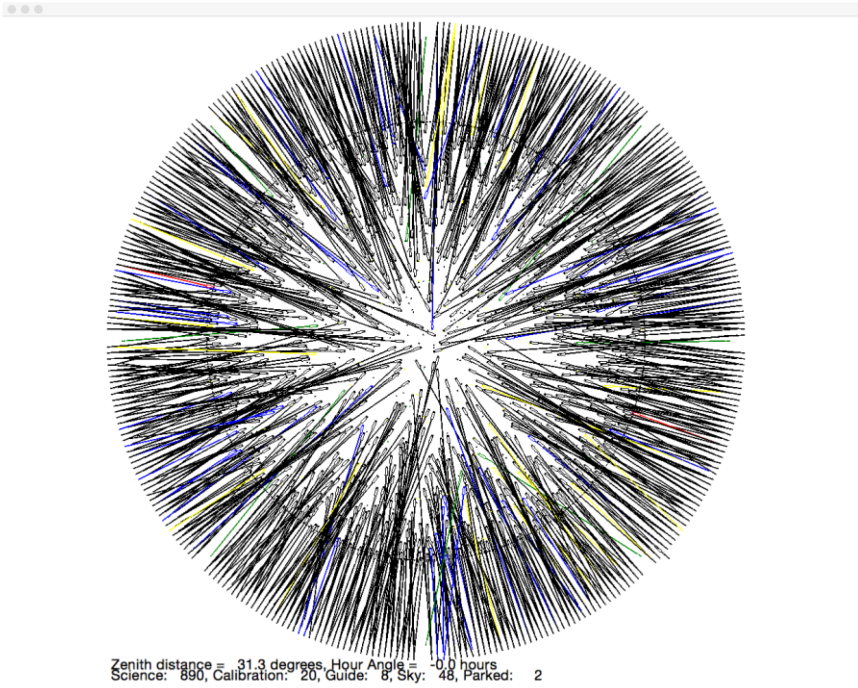

Figure 4 The simulation result of the target acquisition. The black circle middle of the configured field represents the optical field of view. Coloured fibres are sky (blue), calibration stars (yellow), guide stars (green) and unused (red).

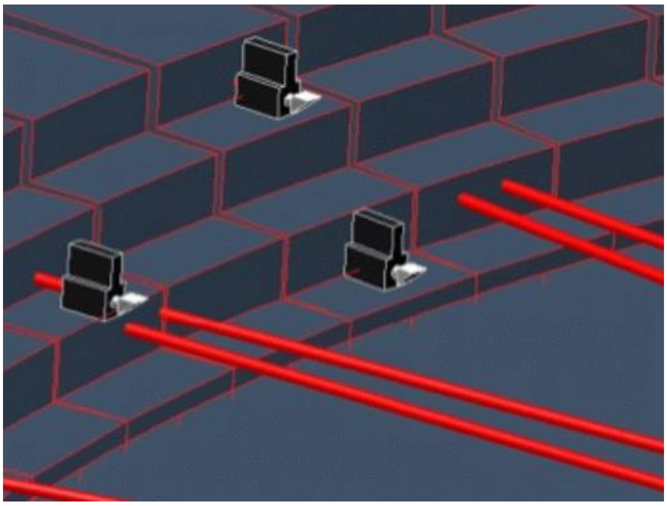

Figure 5 Organisation of the fibres at the edge of the focal plane with three different parking heights. [Dalton et al., 2010] This is zoomed in the part of MOS fibres, the red lines are described the tracks of fibres when they move in the positioner.

WEAVE will operate in three different modes: Multi-Object Spectroscopy (MOS), Large Integral Field Unit (LIFU) and Mini Integral Field Units (mIFU). In MOS mode, all 960 fibres can be moved to obtain the spectra of separate targets at the same time, with a fibre core-size of 1.3 arcseconds on the sky. The LIFU spaxel size is 2.6 arc seconds so this mode is lower resolution, although it has large single bundle, the size being 1 x 1.5 arc minutes for the whole unit. Each of the 20 mIFUs consists of 37 fibres in a close-packed hexagonal array; these are the same fibres as the MOS mode.

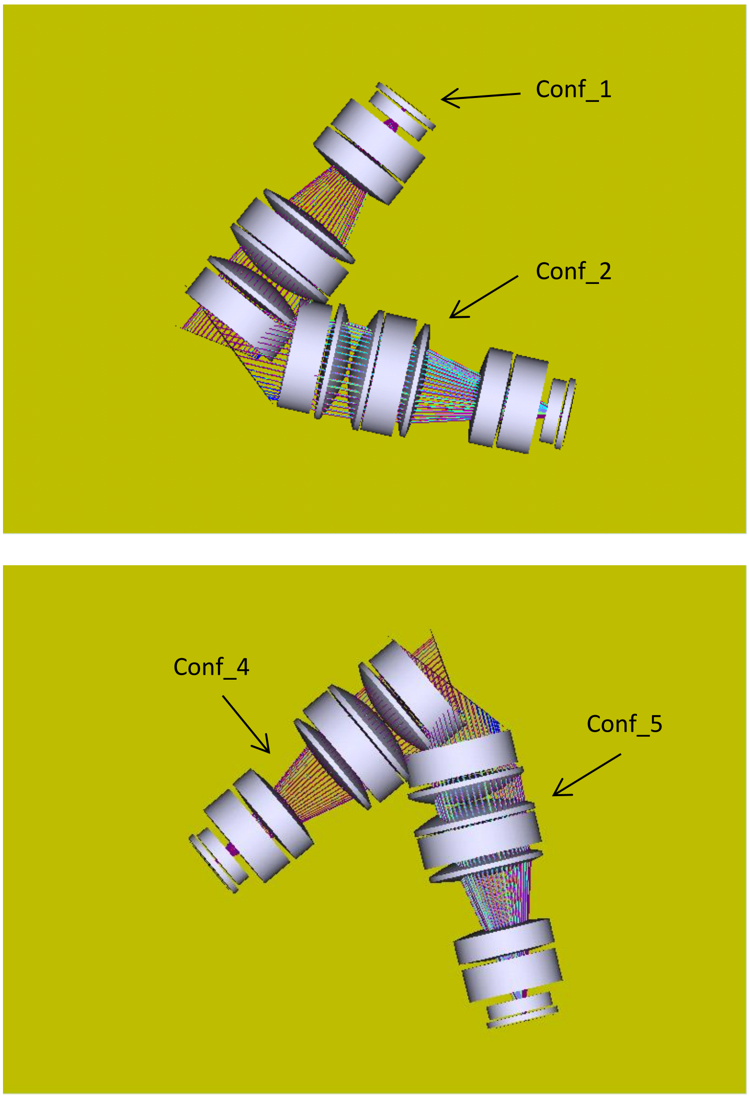

Figure 6 3D layout of the WEAVE camera design. (Top) configurations 1 (low resolution, blue band) and 2 (high resolution, blue band); (bottom) configurations 4 (low resolution, red band) and 5 (high resolution, blue band) This is only for describing the cameras position when it sets in the aimed configuration, each camera sets rotate through the rail along the configurations are changed.

The conceptual design has been developed to fully satisfy the objectives and cost-efficiency. The basic specifications of the WEAVE spectrograph are shown in Table 2 [Rogers et al., 2014] and the optical layout is given in Figure 6 above.

Table 2 Basic specifications of the WEAVE optical system

Parameter	Value
Fibre Core Spacing	1.47x (buffer-limited)
Collimator FOV	+/- 7.3 degrees
Grating angle	23.6 degrees
Camera f/ratio	1.8
Camera diagonal FOV	+/- 12.125 degrees
Core image size	4.19 pixels
Core image spacing	6.16 pixels
Nominal resolution	5004
Blue coverage	366-545nm
Red coverage	579-959nm
Resolution variation for R=5000 at band centre (low resolution) mode	4566-7500
Resolution variation for R=20000 at band centre (high resolution) mode	14500-24000

The spectrograph has a dual-beam design, which incorporates a dichroic at around 600nm; the line densities of the VPH gratings at R~5000 are 1368 in the blue arm and 848 in the red arm. This spectrograph concept was developed from the OPTIMOS-EVE spectrograph after considering the cost-performance benefits of six possible designs; the basic goal is to minimise the total number of spectrographs for the design multiplex by maximising the total wavelength coverage.

The WEAVE optical system allows a total of five different configurations with different wavelengths and resolutions. Configurations 1, 2 and 3 are for the blue channel and 4 and 5 are for the red channel. The wavelength coverage from 366 to 606nm is for configuration 1, 404-465nm for configuration 2 and 473-545nm for configuration 3. Configurations 2 and 3 share the same band and ray path, as is clear from the 3D layout model above; in fact, configuration 3 is a second high resolution band, so the position of the grating after the optical train has not been changed to compare it with the position for configuration 2. The wavelength coverage for configuration 4 is between 579 and 959nm and from 595nm to 685nm for configuration 5. The positions of the cameras can be checked with the change in configuration in Figure 7 below. As the angle of the diffracted beam from the grating is changed, the beam path is changed after the grating, so finally the camera is located in a different position, as in Figure 7.

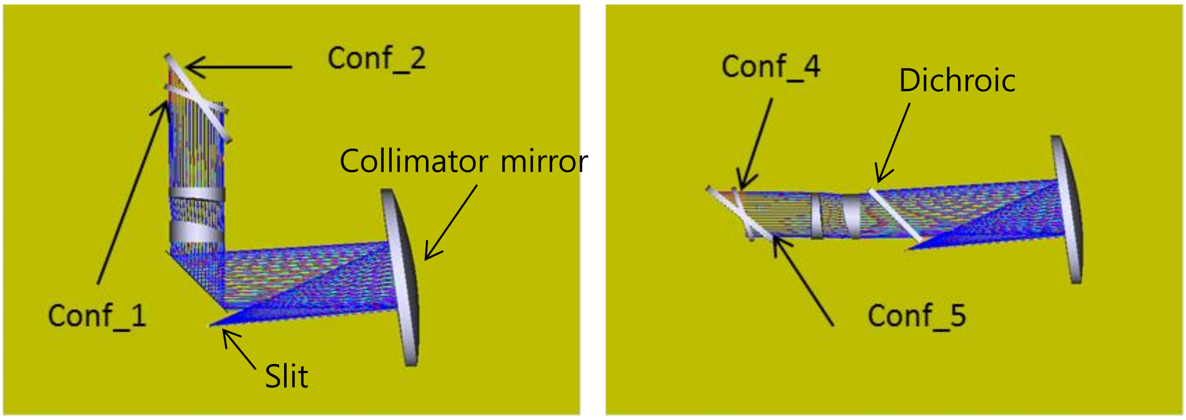

Figure 7 3D layout of WEAVE optical train. VPH grating behind the dichroic and two collimator corrector lenses changes an angle to trace rays in each configuration.

Figure 8 shows an overview of the opto-mechanical design of WEAVE as developed by the NOVA group at ASTRON in the Netherlands [Agócs et al., 2014; Dalton et al., 2014]; the camera parts are located behind the optical train and dichroic filter in both low and high resolution.

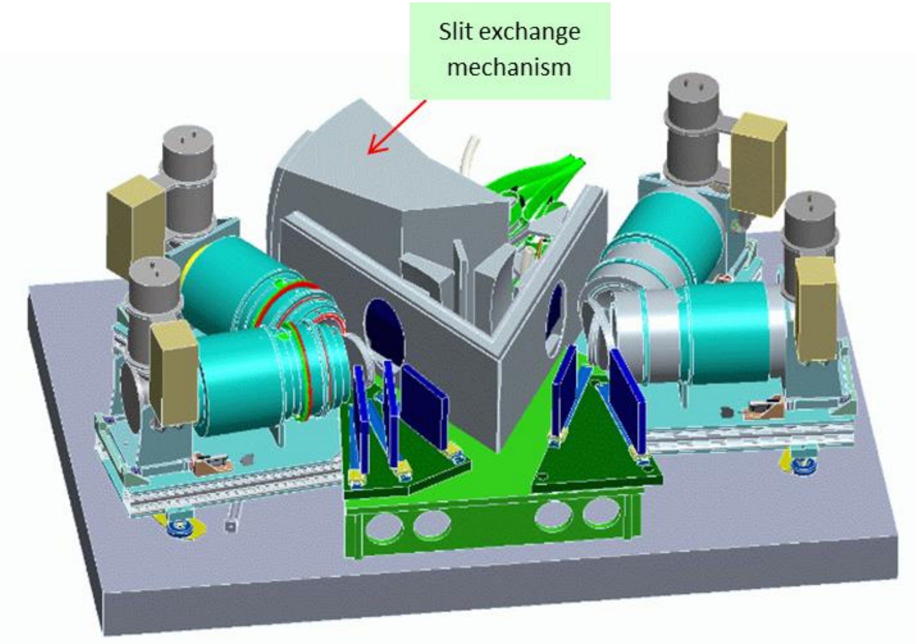

Figure 8 3D layout of the opto-mechanical system of WEAVE. The slit exchange mechanism is located behind the optical train and filters. The position of cameras overlapped in both low and high resolution mode.

1.1.3 WEAVE optics design in Zemax

The early design for WEAVE was developed in CodeV and there was a need to translate it into Zemax. The early design, which is shown in Figure 9, was inspired by another spectrograph for the E-ELT [Navarro et al., 2010], as explained above; however, the current design was developed originally in Zemax. The old and new designs have differences in several parts; for example, the original detector format was a pair of 3k spatial and 8k spectral chips, but these chips proved difficult to procure, and so now the focal plane is divided into two parts with a pair of 6k x 6k CCDs (6k total for spatial direction and 12k total for spectral direction) with a gap in the spatial direction. This change of design has several advantages for the development of the instrument, such as better chip flatness, lower manufacturing cost, and easier availability of spares.

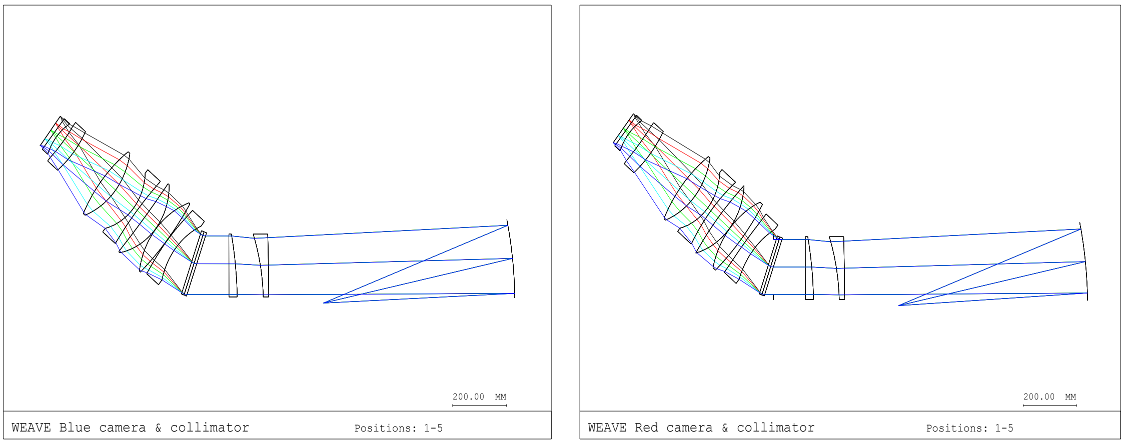

Figure 9 Early design of WEAVE blue camera and collimator (left) and red camera and collimator (right), which was designed in CodeV and Zemax

The other difference is the optical train after the beam splitter; originally this consisted of seven lenses with three aspheres, but it now has eight lenses for each arm and requires only a single aspheric surface. The merit of the new design is also that it allows for easier manufacturing and a lower cost.

The blue band VPH grating ruling density is 1385 lines/mm for low resolution, and 3580 lines/mm for high resolution; the red band VPH grating density is 876 lines/mm for low resolution, and 2431 lines/mm for high resolution [Rogers et al., 2014].

The two collimator corrector lenses in each arm have spherical surfaces, although there is a risk of aberration. The camera lenses consist of a single aspheric (4^{th}, 6^{th} and 8^{th} orders) and identical design for the two cameras, which is changed only for coatings and lens spacing between front and rear. The specifications of the optical components are shown in Table 3.

The entrance 'slit' for the spectrograph is formed by arranging the fibre exits on the source surface, and since the fibres are free to be positioned as we choose, the effective slit is curved in two dimensions to relax other constraints in the optical design. The field positions for x (spatial) and y (vertical) are shown in Figure 10. The x values show only one half of the image plane, so we assume the other half of the plane is identical size in the spectral image simulator. The positions derived from 9 fixed fields of Zemax, the arbitrary points lying on the source surface along with the curve. The values are represented in Table 5 and 6.

Table 3 The specifications of the spectrograph components [Rogers et al., 2014]

Component	Number of components	Material	Finished diameter (mm)	Asphere
Slit lens	1	Fused silica	200 x 30	None
Collimator mirror	1	Zerodur	645 x 260	None
Dichroic (25 mm thick)	1	Fused silica	390 x 308	None
Collimator corrector lens 1	2	Fused silica	330 x 210	None
Collimator corrector lens 2	2	PBM2Y	330 x 210	None
VPH substrate (20 or 25mm thick)	10	Fused silica	220 x 220 or 340	None
Camera lens1	2	PBM2Y	235	Surface 2
Camera lens 2	2	PBL1Y	304	None
Camera lens 3	2	S-FPL51	320	None
Camera lens 4	2	PBL1Y	316	None
Camera lens 5	2	S-FPL51	298	None
Camera lens 6	2	PBM2Y	253	None
Camera lens 7	2	PBM2Y	270	None
Camera lens 8	2	S-LAL9	253	None
Cryostat window (15 mm thick)	2	Fused Silica	180	None

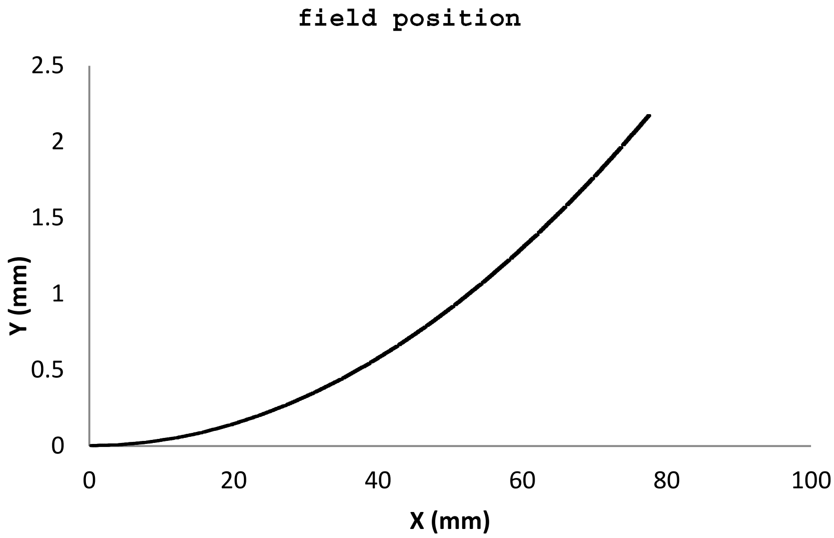

Figure 10 X (spatial) and Y (vertical) field position on the slit

The diagram of the final WEAVE design is shown in Figure 11 below; it passed the optical Final Design Review (FDR) in January 2014. The light from the source, i.e. the fibres, can be traced to the spherical collimator and divided by dichroic beam splitter. The light passes into a blue and red arm after the splitter, and then is dispersed by the VPH grating, finally the light traces into the cameras, which consist of eight different lenses and the window before the final image plane. Each blue and red arm performs in a low and a high resolution mode, so the function of the VPH grating is sensitive to make a focusing the image on the detector through each camera. The VPH gratings are made with fused silica and the thickness varies with the resolution, i.e. 20mm for a low resolution and 25mm for a high resolution.

Unwanted reflections from surfaces within the optical train give rise to stray light and ghosts. The WEAVE preliminary design had an issue due to normally reflected light at the focal plane arriving back at the grating in 1^{st} order, and then being reflected back in 0^{th} order by the grating to form an *undispersed* image back on the detector. (known as a Littrow ghost.) [Burgh et al., 2007] The need to redefine the focal plane to accommodate two 6kx6k detectors implies a small gap somewhere in the middle of the spectral region, and it is possible to steer the Littrow ghost into this gap by designing a slant on the fringes of the VPH grating. The locations of the gaps in the two cameras were determined by the project scientist by consideration of regions of lower interest in the stellar spectra.

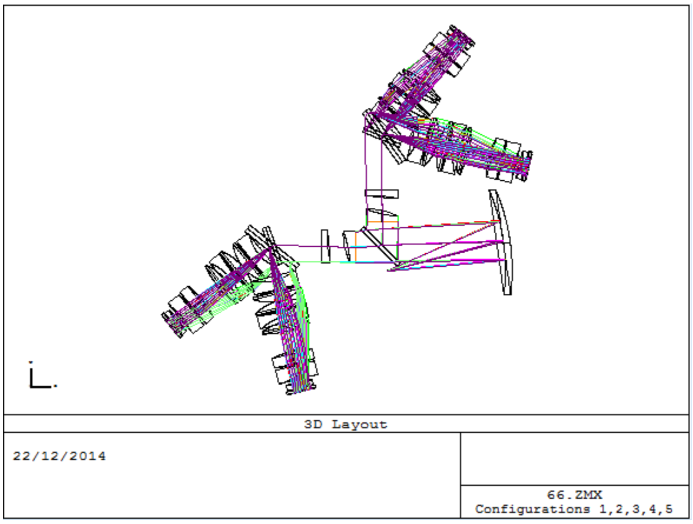

Figure 11 The WEAVE optical diagram with ray tracing in Zemax. It shows the ray tracing resulting at both the blue and red wavelengths.

The estimated system performance for the high resolution mode is shown in Figure 12. Throughput of the final design of WEAVE in a low resolution is above 25% with a wavelength range from 450 to 850nm and in a high resolution is above 20% with a wavelength range from 400 to 690nm.

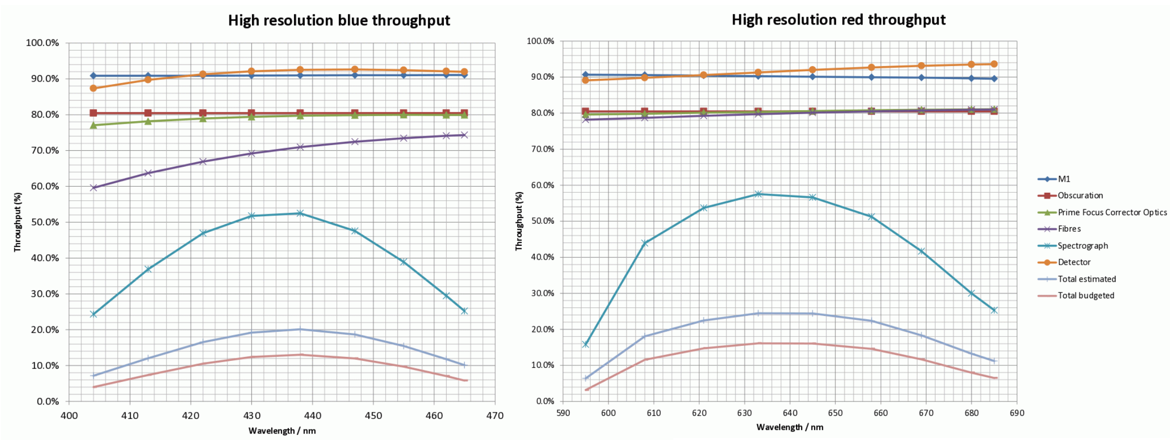

Figure 12 Total system performance of WEAVE. The right graph shows the throughput in high resolution mode for the red arms and the left graph shows the same resolution but for the blue arms. [Dalton et al., 2014]

These graphs show us the individual contributions to the overall performance of the system from the main components of the telescope and WEAVE system. This includes the additional prime-focus obscuration due to the large structure of the fibre positioner, the expected grating performance and the detector quantum efficiency, as well as transmission losses in the optical components. It does not include light loss at the input due to seeing or aperture effects, or field-dependent vignetting terms, which are included explicitly in the simulation later.

1.2 WEAVE imaging process review

Zemax software is a powerful tool for analysing the performance of an optical system by ray tracing and optimising the system with the required performance, as part of the detailed system design. We have used Zemax to establish the data for developing the simulator for the WEAVE imaging process. The simulator will be developed in several parts, using Zemax to determine a multi-wavelength grid of monochromatic images of each fibre core within the spectrograph. The other elements of the system performance such as the telescope, corrector, atmospheric effects and target information will be calculated in the simulator itself. The details of the Zemax work will be explained in the next chapter.

Chapter 2

THE WEAVE WORK FLOW AND PRE-STUDY FOR IMAGE PROCESSING

2.1 Purpose of the study

The completed WEAVE optics design was delivered in 2014. Here we aim to verify that the performance matches the various system requirements. The purpose of the study is to generate simulated data to allow the verification of the whole data reduction and analysis pipeline and also to generate the high signal-noise reference images that can be used as fitting templates for the extraction and analysis of the final science spectra. Further step is making own simulator for WEAVE, this is the pre-study and generating data sets for the simulator.

2.2 PSF data generation using Zemax

Zemax is commercially available optical design software that can be used to develop optical instruments and check performance details by ray tracing with various environments and user constraints, and support tools to optimize performance [Zemax, 2011]. Zemax provides large-scale ray tracing of the optical system with detailed parameters for all components and apertures from the source to the image plane, i.e. the detector.

The Zemax design of WEAVE has 5 configurations along the position of the cameras, for high and low resolution, 1, 2 and 3 are the blue band and 4 and 5 are the red band as explained in the previous chapter. For the optimization of each configuration we defined 9 wavelengths and 9 fields covering the range of slit heights as given below at Table 4 and 5.

Table 4 Wavelengths (μm) for each configuration used for generating flux data

Wavelength	Configuration				
	1	2	3	4	5
1	0.366	0.404	0.473	0.579	0.595
2	0.390	0.413	0.483	0.629	0.608
3	0.424	0.422	0.493	0.678	0.621
4	0.457	0.430	0.503	0.727	0.633
5	0.490	0.438	0.513	0.775	0.645
6	0.520	0.447	0.523	0.822	0.658
7	0.549	0.455	0.533	0.869	0.669
8	0.578	0.462	0.543	0.914	0.680
9	0.606	0.465	0.545	0.959	0.685

Table 5 X and Y Field positions for generating flux data

Fields	X(mm)	Y(mm)
1	0	0
2	9.689375	-0.034
3	19.37875	-0.13608
4	29.06813	-0.30637
5	38.7575	-0.54487
6	48.44688	-0.85159
7	58.13652	-1.22652
8	67.82563	-1.66965
9	77.515	-2.181

Table 6 Setting x and y points for getting flux data

X point	position	Y point	position
setxfields (1) =	0.08085	setyfields (1) =	-0.0001637
setxfields (2) =	0.2423	setyfields (2) =	-0.0004909
setxfields (3) =	0.4038	setyfields (3) =	-0.0008188
⋮	⋮	⋮	⋮
setxfields (478) =	77.12	setyfields (478) =	-2.159
setxfields (479) =	77.28	setyfields (479) =	-2.168
setxfields (480) =	77.44	setyfields (480) =	-2.177

First, each point on the final plane has to be indicated to get the data as arbitrary x (spatial) and y (vertical). Spatial direction is intended to describe normal x-axis, because we aim to study the PSFs data on the image plane in this step, the images from the source are shown along the x axis and it's related with a resolution. Therefore we call the x axis the spatial axis and the y axis is vertical axis. The size of the slit surface is 77.44mm(spatial) ×2.177mm(vertical), so it can be divided about 0.16 for x and 0.00032 for y to make 480 points for each direction.

Now we have an array with 480 data points, corresponding to the position of each fibre on the detector. In the final run of the ray tracing we replaced these 'arbitrary' points with the nominal mechanical positions of each fibre within the slit blocks, as generated by the NOVA group [Agócs et al., 2014].

The Zemax function we used is the Geometrical Image Simulation; there are several parameters we need to decide for getting the proper result of the ray tracing simulation. Choosing how many rays to generate at the same time for single image in the simulation directly affects the run-time. The specific parameters are shown in table 7 as below. The size of one pixel in the final plane is 15μm, so total image size is 0.315μm for 21 pixels each.

Table 7 parameters for geometric image simulation

parameters	**value**
Field size	0.085 μm
Image size	0.315 μm
File	CIRCLE.IMA
Rays*1000	1000
Show	Grey Scale/false colour
Source	Uniform, circle
Number of Pixels	21
NA	0.0000
Total Watts	1000.00
Configuration	Current
Reference	Chief Ray

Also we eliminate vignette rays in the system, according to Geometrical Image Analysis Setting in Zemax, there are two different entry to reflect vignetting factor in the simulation, 'remove vignetting factors' is irrelevant for this system so we apply only for 'delete vignetted'.

As we have to change fibre number (field), wavelength and configuration for each trial of simulation, Zemax provides a useful macro language for this work. The macro includes 9 wavelengths for each configuration as it shows at table 4. Then the macro file is completed by some commands using the Zemax program language, the main program is shown below.

The SYSP command means 'SETSYSTEMPROPERTY' and it's for setting properties of the system such as field, wavelength, ray intensity, polarization etc. The meaning of the number is 'the field number' and it can be allocated x, y coordinate to each number. For example, the wavelength in micrometers can be decided using number 202. The fibre-core source of the rays is indicated by the IMA file to simulate a geometric image convolving the actual point-spread function with the chosen input source geometry. For this study we use a simple filled circle image to represent the fibre core. The output file is selected using the GETTEXTFILE command, with designated parameters as the table 7. This produces a file with a pixelated grid of intensities, centred on the peak of the PSF. In the same way we must also produce a footprint file from the same command to determine the actual image position on the final plane.

```
FOR wave2, 1, 9, 1
    FOR fiber, 1, 480, 1
        fiber_x = setxfields(fiber)
        fiber_y = setyfields(fiber)
        SYSP 102,1,fiber_x
```

```
            SYSP 103,1,fiber_y
        WAVE = SETWAVES(5,WAVE2)
        print WAVE2,WAVE
        SYSP 202,1,wave

        fileout$ = fileout1$ + $str(wave) + "_" +$str(fiber_x) +"_" +$str(fiber_y)
        fileout$ = fileout$ + ".out"

        GETTEXTFILE fileout$, IMA

        NEXT
NEXT
```

The final results from Zemax simulation is shown in Figures 13 to 17, as the PSF images at the focal plane using the parameters set in Table 7.

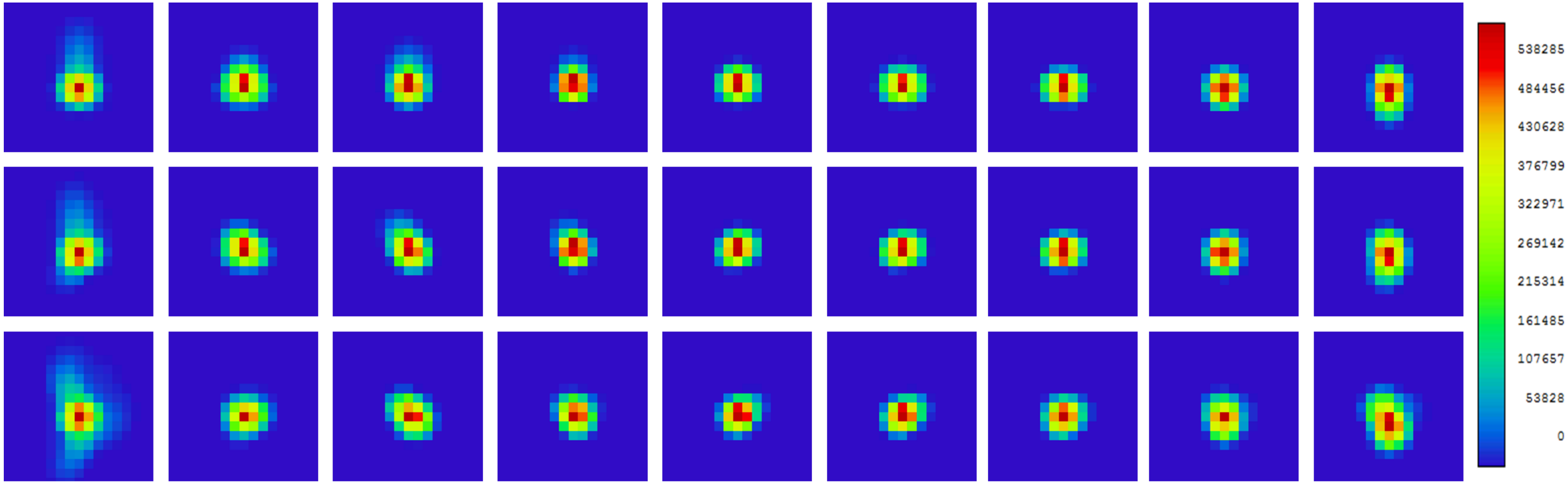

Figure 13 The images of the focal plane from geometric image analysis. These images are for configurations 1 of 5, i.e. LR blue. The first row shows the images at field (0,0), i.e. field 1 from table 5, and fields 5 and 9 follow. The 9 wavelengths are from 0.366μm to 0.606μm of configuration 1 in Table 4.

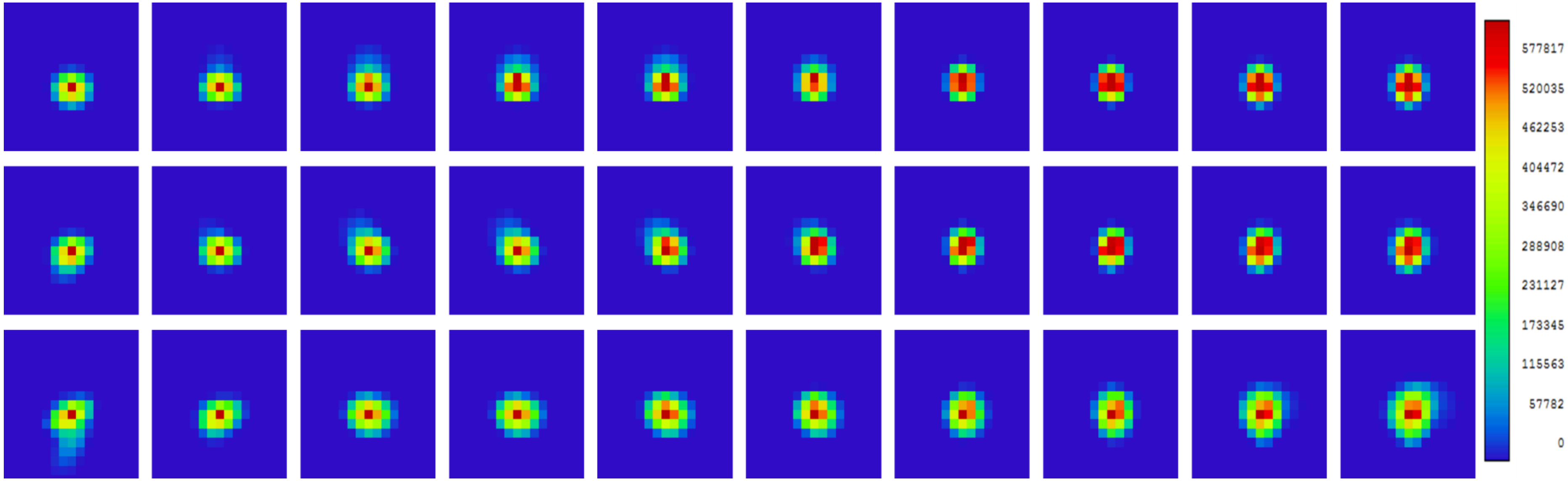

Figure 14 The images of the focal plane from geometric image analysis. These images are for configurations 2 of 5, i.e. HR blue. The first row shows the images at field (0,0), i.e. fields 1 from table 5, and fields 5 and 9 follow. The 9 wavelengths are from 0.404μm to 0.465μm of configuration 2.

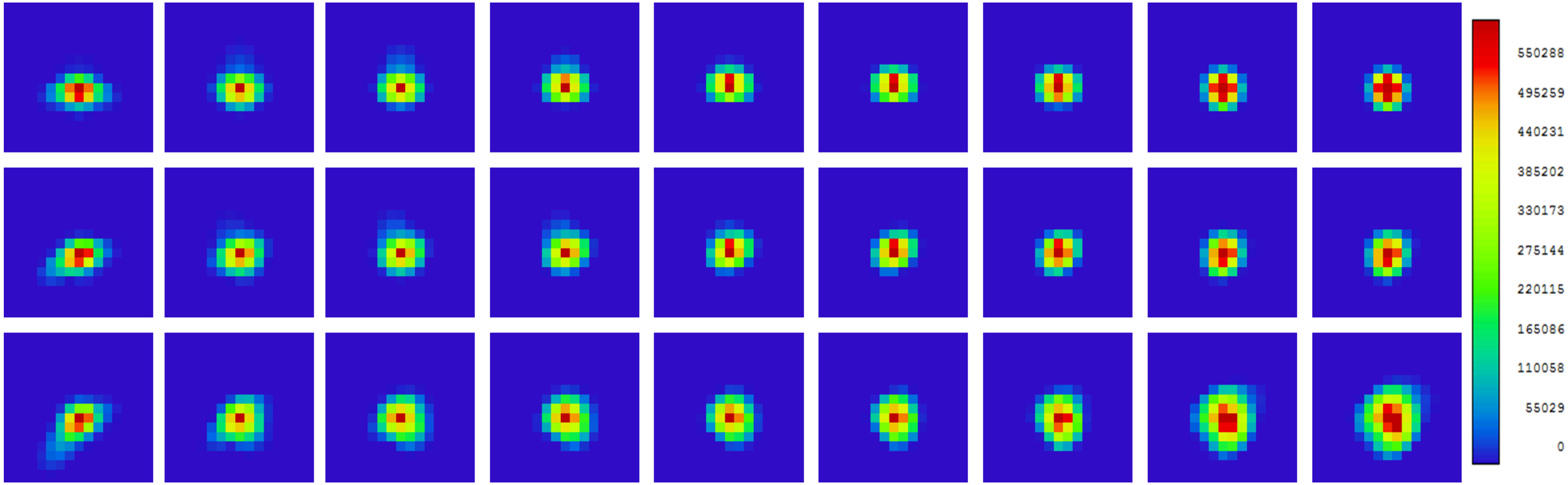

Figure 15 The images of the focal plane from geometric image analysis. These images are for configurations 3 of 5, i.e. HR blue. The first row shows the images at field (0,0), i.e. fields 1 from table 5, and fields 5 and 9 as follow. The 9 wavelengths are from 0.473μm to 0.545μm of configuration 3.

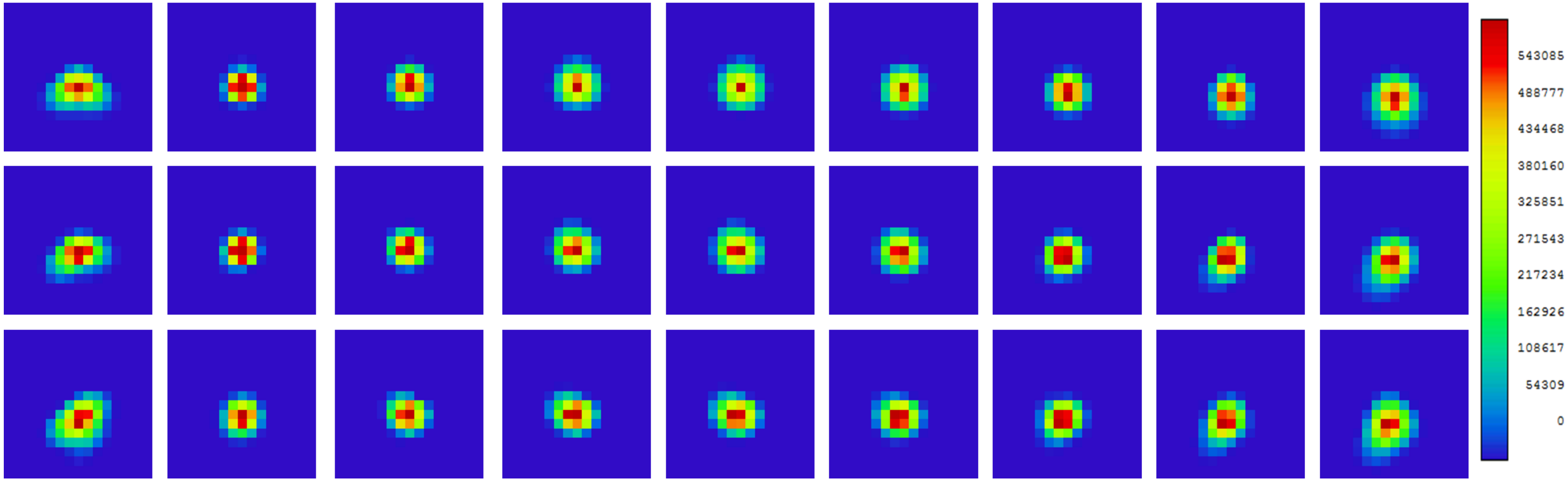

Figure 16 The images of the focal plane from geometric image analysis. These images are for configurations 4 of 5, i.e. LR Red. The first row shows the images at field (0,0), i.e. fields 1 from table 5, and fields 5 and 9 follow. The 9 wavelengths are from 0.579μm to 0.959μm of configuration 4.

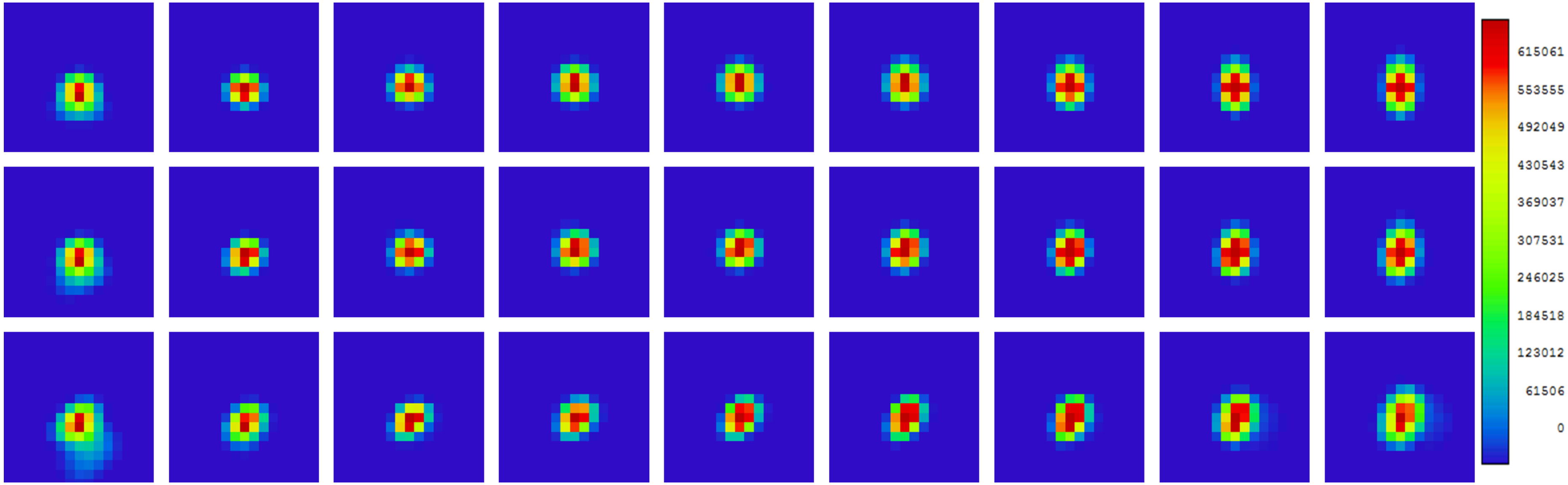

Figure 17 The images of the focal plane from geometric image analysis. These images are for configurations 5 of 5, i.e. HR Red. The first row shows the images at field (0,0), i.e. fields 1 from table 5, and fields 5 and 9 follow.,The 9 wavelengths are from 0.595μm to 0.685μm of configuration 5.

2.3 Summary and Conclusions

We explained how we generate PSF data at the focal plane of the WEAVE spectrograph system. Zemax is key software to do raytracing and image analysis and finally obtained 21,600 datasets (9 wavelengths*5 configurations*480 fields) for PSFs and footprint locations. Each data set is a 21 by 21 grid of effective CCD pixels. With these dataset, we can now use these results to develop a general image simulator for testing the final WEAVE data pipeline.

In terms of the Zemax simulation, the source for the ray tracing can be generated by random sampling of many thousands of individual rays. In this part of the study we have restricted ourselves to the details only of the optical system performance. Additional inputs, such as the detailed throughput of the different system components and grating performance will be added in the next step.

The final results of the Zemax modeling are presented above in Figures 13 to 17, we can see the PSFs images on the final plane change in a complex but systematic manner as we move along the trace of each fibre. These changes will have a significant effect on the precise spectral resolution that can be obtained from each fibre at each wavelength. Moreover we can think about the image crosstalk between adjacent fibres, as this is important topic related to the final image processing.

As we want to simulate the instrument performance at all wavelengths, configurations and fields i.e. fibre numbers- we need to use Zemax macros for these repetitive works, but will aim to interpolate the PSFs between the grid points given here. As a check of the image fidelity in the middle of the simulation, we confirm the footprint data as shown at Figure 18. Footprint of image simulation simply indicates the beam size and then we can get the size from the boundary with any directions, x and y. Also the result file includes the information about the location in the field, i.e. the center of the images. In the Figure 19, this is the footprint data only for x and y center for configuration 2, the values are increased smoothly so we have a good indication that the full data set does not contain any deviations from these data points during finer sampling. Thus we conclude that the initial grid presented here is a good enough starting point to apply to the next step for WEAVE image processing.

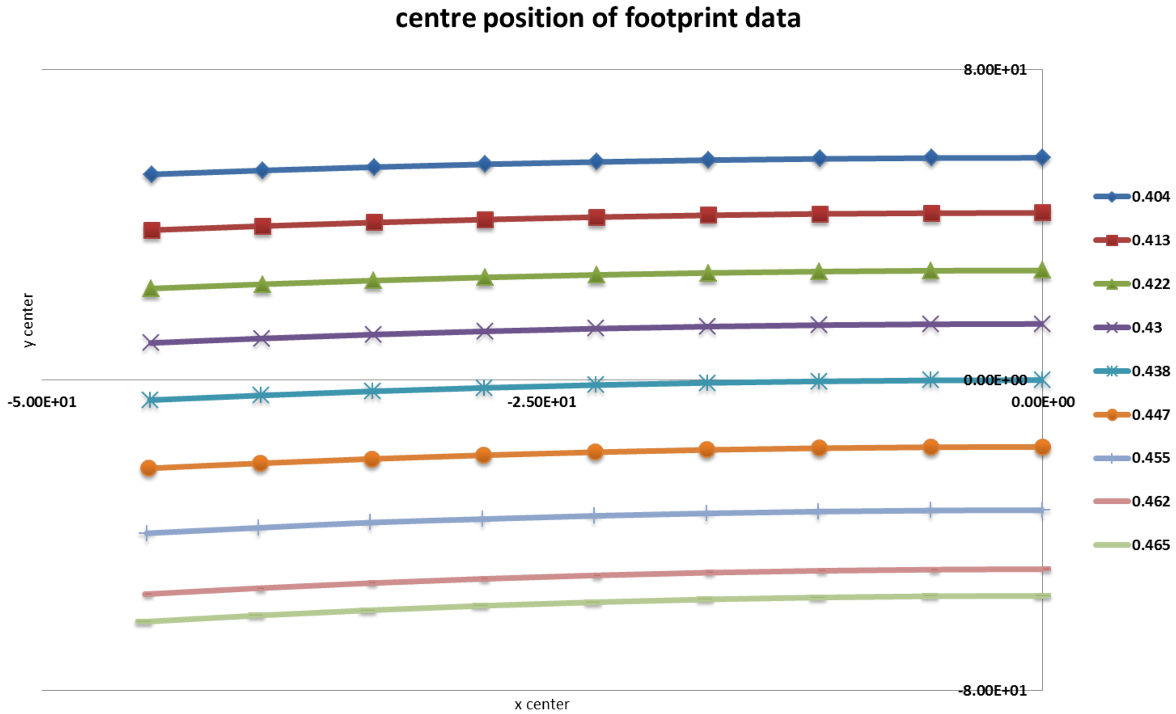

Figure 18 Footprint data for configuration 2. This is only for x and y center of the data for 9 wavelengths.

Chapter 3

THE WEAVE END-TO-END SPECTRAL IMAGE SIMULATOR FOR DATA PROCESSING

3.1 WEAVE data flow

3.1.1 Purpose of the study

The main purposes of this study are to accomplish the following objectives: 1. Verify and validate the WEAVE data flow. We have to check the data reduction, calibration, and analysis pipeline before the operation starts and use the simulated data. This work is included in level 1 of WEAVE CPS. 2. By doing this, we can provide the pipeline team with high signal-noise reference images as fitting templates for the fibre positions and the PSF mapping. Given

PSFs data from Zemax from the earlier simulation before this study, we can compare the results to each other to prove the performance of the designed WEAVE optical system and finally predict the products once WEAVE operates in the future.

3.1.2 Overview WEAVE survey

Once WEAVE begins operating, there will be a substantial continuous flow of new data; consequently, it is necessary to validate whole data flow and the procedure as end-to-end simulation. The WEAVE science processing and archiving (SPA) is a subsystem of the WEAVE project being developed at Cambridge (CASU) and the Canary Islands for archiving and providing the observation data to the users and for building and analysing the WEAVE data products. It has several levels to deal with a large data set as follows [Walton et al., 2015; Walton et al., 2014].

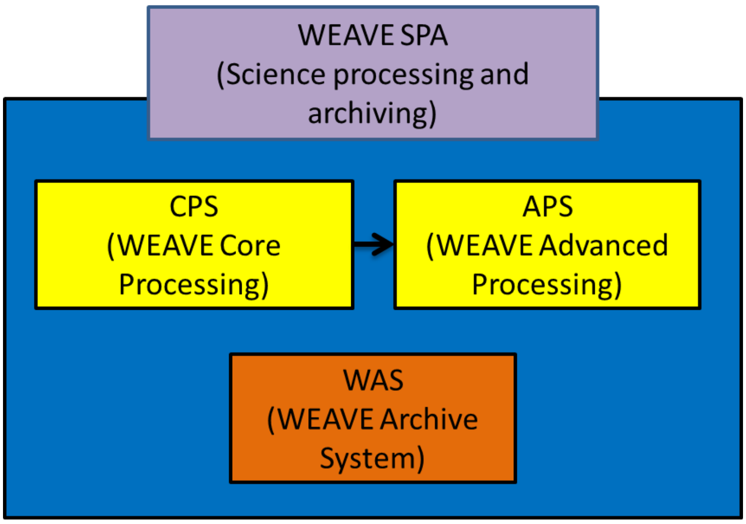

Figure 19 Simple diagram of WEAVE pipeline.

The raw data files from the instrument will be processed through the WEAVE Core Processing (CPS) pipeline at CASU and then passed to the WEAVE Advanced Processing (APS) pipeline (at the IAC) for determining scientific outputs from the data, such as classifications, redshifts, radial velocities, and abundance information from the high resolution spectra. All results from CPS and APS will be passed into WEAVE archive system (WAS, operated at the Italian Telescopio Nazionale Galileo, TNG) and will be released to the users via the archive user interface.

The specific steps of data flow are presented as below [Walton et al., 2015].

- Level Q: quick-look analysis (to be run at the telescope as required)
- Level 0: basic data quality control checks
- Level 1: full image processing and spectral extraction
- Survey progress monitoring
- Level 2: higher level science analysis
- Archive systems

Level Q, Level 0, and Level 1 are built by the CPS system and will run afterward; also, all the data flow will be controlled from Survey progress monitoring in CPS. Level 2 is carried out in the APS system.

The whole procedure of WEAVE data flow is shown in Figure 20 as shown below.

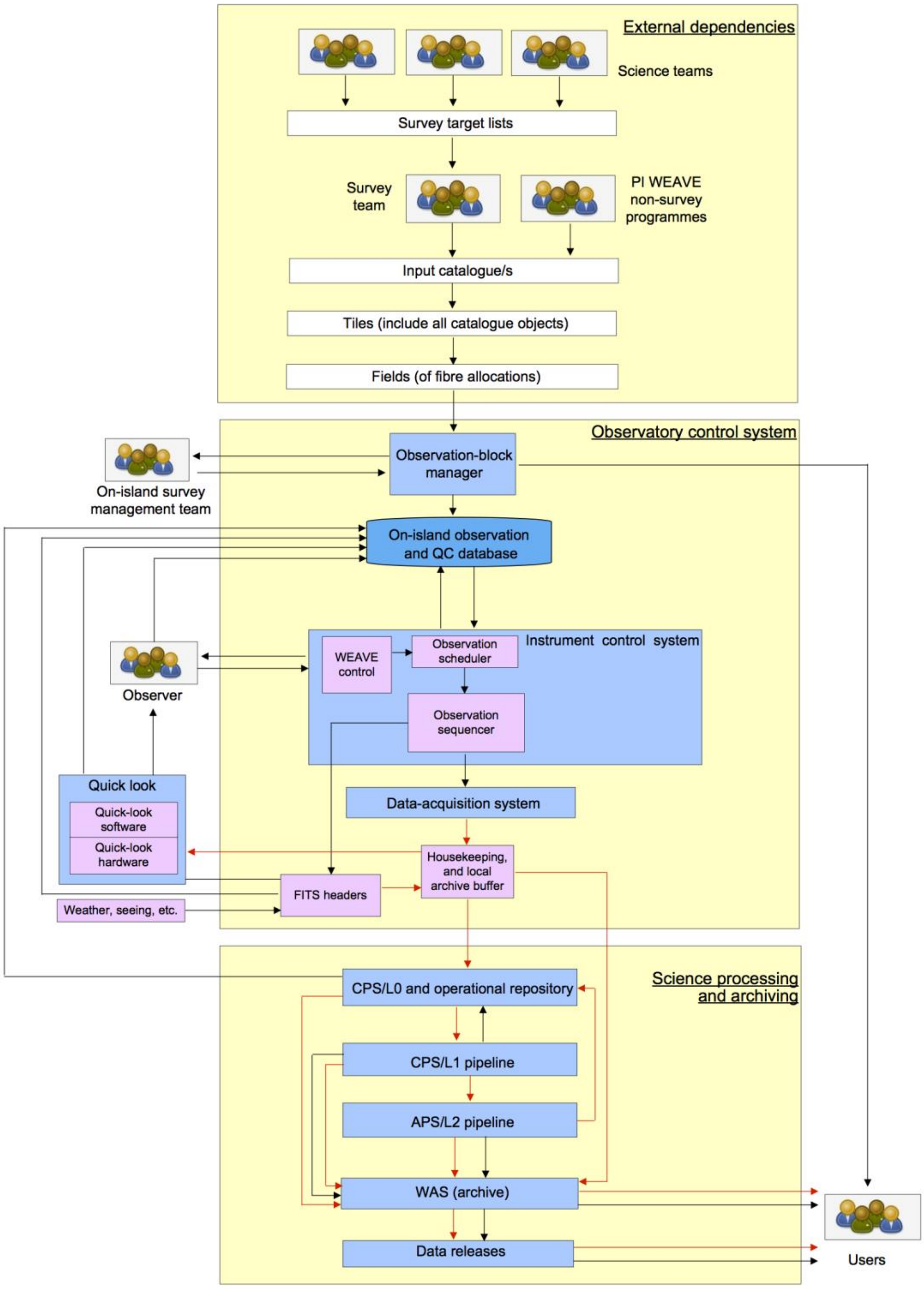

Figure 20 WEAVE data flow. Each block of procedures represent various elements of the WEAVE science processing and archiving system (SPA) [Walton et al., 2015].

3.2 Simulator for WEAVE image processing overview

There are many first order requirements that were input to the optical design such as wavelength coverage, limit on stray light level, and the characteristics/capabilities of the detector. The key requirements among these are resolution, crosstalk, and throughput. In the early design phase, these specifications were calculated and simulated in various conditions and are represented in Figure 21 that shows the map of low/high resolution for each blue (top) and red (bottom) arm. The resolution map consists of the result produced by a massive ray tracing at multiple slit positions and wavelengths, we extract a 1D spectral line from the values on the final image plane and then calculate the FWHM of the line. The effective resolution is then determined from the data using a Rayleigh criterion. From these figures we can get an indication of the performance of the instrument, although the figures indicate that the variation of resolution is somewhat complex. A full end-end WEAVE image processing simulator is therefore a key component to determine the real performance of the instrument as applied to model observations.

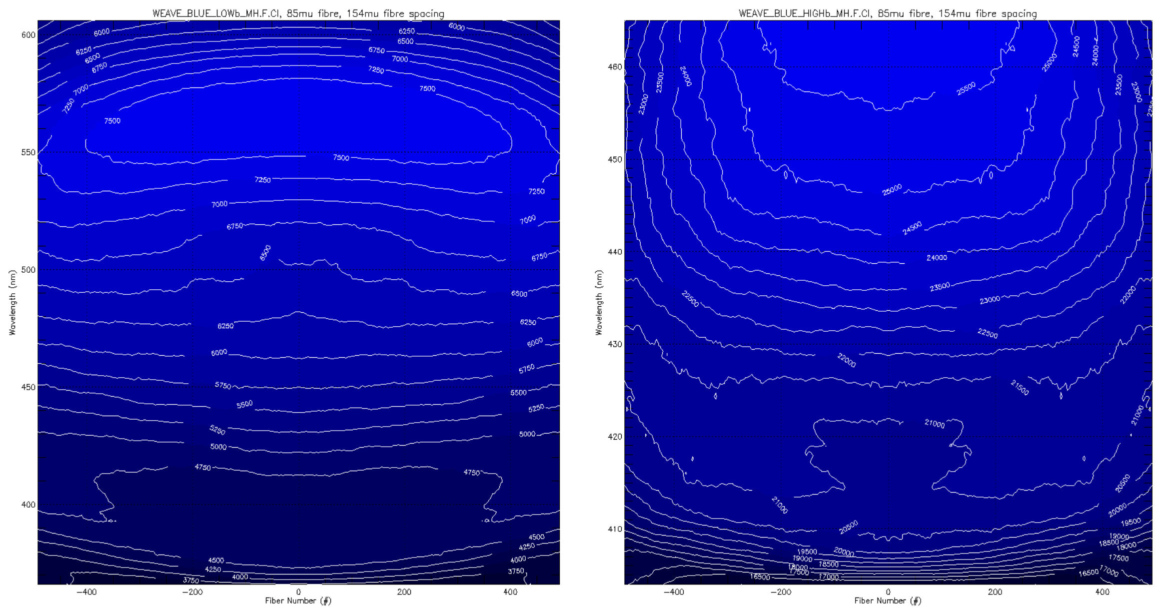

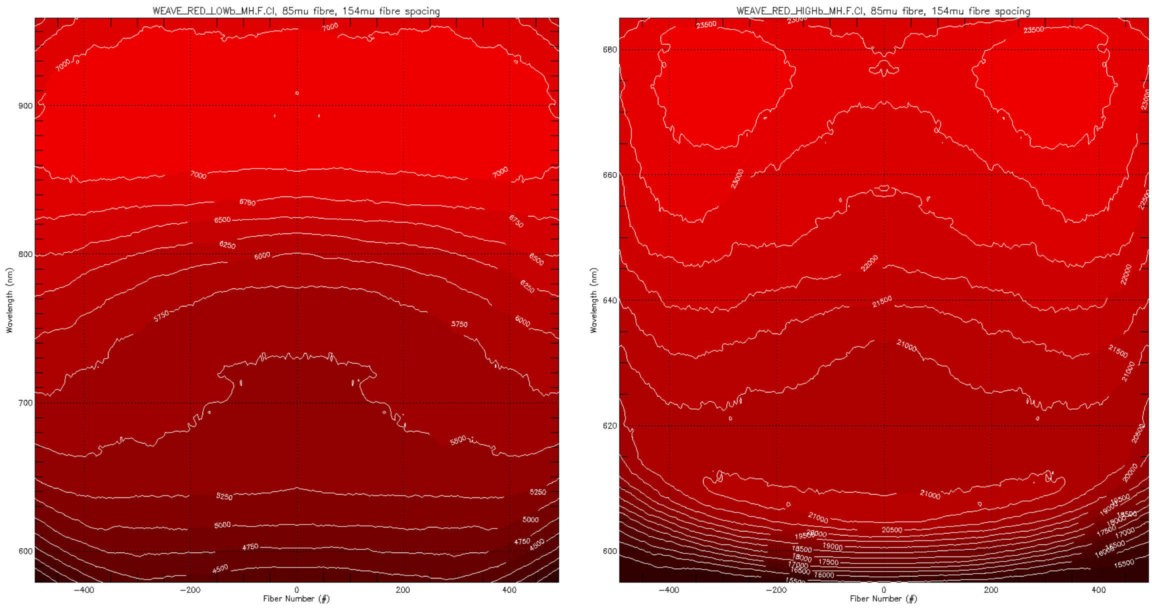

Figure 21 Low and high resolution map blue (Top) and red (Bottom) arm [Rogers et al., 2014]

As shown in Figure 19, there are two major elements of the processing pipeline: CPS calibration pipeline and APS science pipeline [Irwin et al., 2015]. The calibration of the data follows a general procedure to remove the instrumental signature from the observed spectra. The list of pipeline calibration steps is represented as below.

- Electrical crosstalk correction

  Electrical crosstalk occurs for multi-channel detector systems; for example, the signature of the image from one detector can be read out to the other detector, which means that a component of the false signal cannot be removed from the data. It can also occur with single detector with two amplifiers when a ghost image contaminates the detector. Using an arc lamp, we can find the scale factor for an individual instrument, and this is related to the unique characteristics of the system. The simple form of crosstalk matrix C_{jk} in equation 1 is a general term for any calibration procedure, which has to be monitored monthly because the system capabilities constantly change during ongoing operation.

$$I'_j = I_j - \sum_{k \neq j} I_j C_{jk} \quad (1)$$

- Linearity correction

  As the CCD characteristic is non-linear, we need to determine a correction to linearise the system response.

- Bias combination

  This is one of compulsory steps to adjust zero default before starting observation of any target. The bias usually will be removed from the science frame after being exposed for zero seconds, or we can use mean level of bias frame by multiple exposures to the bias frame.

- Dark combination

  Dark current is a usual element to be corrected from any electrical equipment such as detector, and it can be subtracted from the frame after bias correction. The mean dark current value is related with exposure time. The D(x,y) in equation 2 is the mean dark frame.

$$F'(x,y) = F(x,y) - \Delta t D(x,y) \quad (2)$$

- 2d flat field correction

  This correction is able to correct the detector response by uniform 2d field illumination such as a dome flat, but this does not provide the true detector response for a fibre instrument. The detector response can be determined independently of the fibre train by using a series of different monochromatic LEDs located within the spectrograph in front of the focal plane.

- Scattered light correction

There are two contributions to stray light within the system: true scattered light from optical surfaces within the instrument, and optical crosstalk due to the overlapping profiles of adjacent fibres at the detector. It is therefore critical to be able to determine the PSFs of adjacent fibres independently, particularly given that in the science data we expect to be observing targets with up to five magnitudes of dynamic range in brightness.

For getting characteristics of the PSFs, WEAVE will use a 'salsa flat' observation, which is looking at a full-field flat lamp exposure with only every third fibre illuminated [Irwin et al., 2015]. We can thus determine the fibre profiles in terms of the true PSF, Ψ(x,y) When we get the profiles for every required wavelength, we can determine what fraction of the flux for one spectrum, may be contaminating its neighbour.

Basically, the PSF can be represented by a basic Sersic distribution such as Equation 3 [Sersic, 1963]; I_0 is central surface brightness and n is Sersic index, which is determined by curvature of the brightness profile.

$$I(\mathrm{R}) = I_0 e^{-(b_n (\frac{R}{R_e})^{\frac{1}{n}})} \qquad (3)$$

$$\psi(\mathrm{x}, \lambda) = \psi_0 e^{-(\frac{|x-x_0|}{\omega})^{\alpha}} \qquad (4)$$

The value of the flux at given wavelength and fibre is

$$\mathrm{S}(\lambda) = 2\int_0^{\infty} \psi(x,\lambda)dx = \frac{2\psi_0\omega}{\alpha}\Gamma(\frac{1}{\alpha}) \qquad (5)$$

- Arc exposures

  Arc lamp exposures are part of the procedure for wavelength calibration. Using above process, we can gather the value of aperture mask as a fibre profile; therefore, the arc spectra can be calculated from the aperture mask.

- 1d flat correction

  Using salsa flats, we can get individual fibre profiles, i.e. clear PSFs without crosstalk effect from adjacent fibres. We can use this information to normalize science spectra by dividing 1d flat spectrum, and we know the characteristics of each fibre when they are illuminated by strong light source and obtain the fibre throughput.

- Sky background correction

  The sky background also includes 1) Unresolved stellar light, 2) Gas emission lines, 3) Atmospheric features, and 4) Solar light from any moon phase.

The other element of the CPS Level 1 is CPS science pipeline, which is for the calibration of 1d spectra from the 2d science exposures. The following figure is the data flow of CPS science pipeline [Walton et al., 2015].

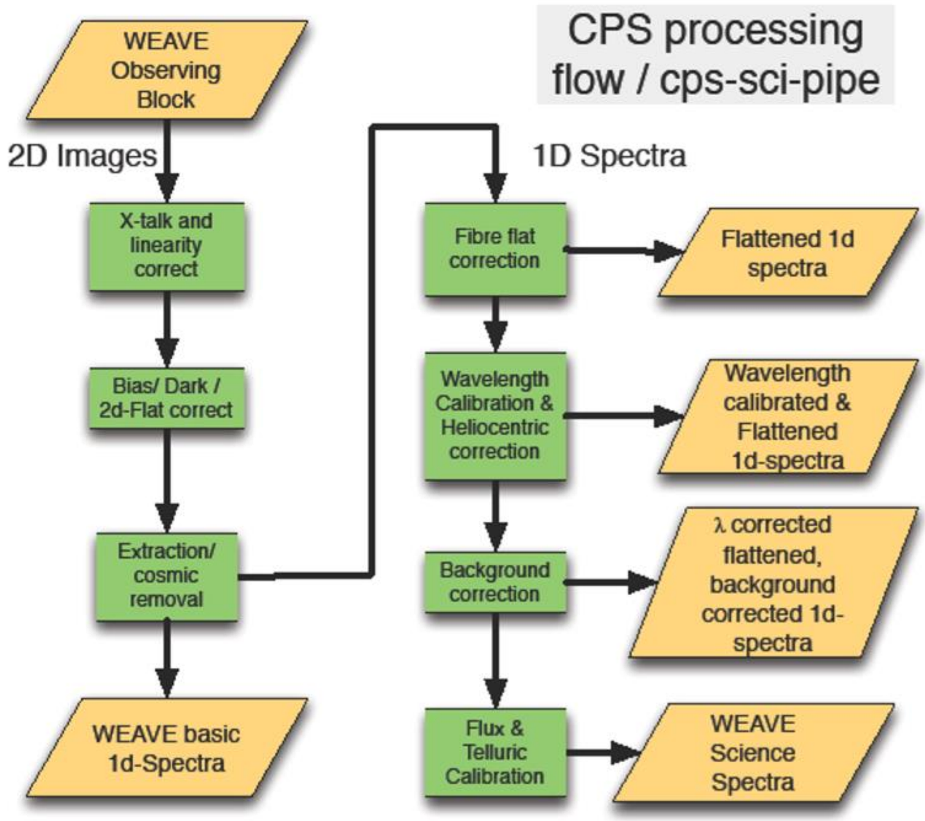

Figure 22 CPS processing flow for science pipeline. 2D images from observation pass to the 1d spectra procedure; they can be used for calibration, various correction steps, and science spectra [Walton et al., 2015].

3.3 Method - Spectral image modelling

The image simulation is divided into two parts: Zemax ray tracing simulation, which was discussed in the previous chapter and regenerating science spectra from sample data for a case study. We generate PSFs and footprint data for a set of discrete wavelengths and each given spectrograph configurations for 480 individual input fibre positions (referred to as fields earlier in Zemax). The Zemax files have five configurations: three high- and two low-resolution. For each configuration, we sample the PSF for nine wavelengths for each input fibre position to yield an image map and centroid position. Each PSF is sampled on a 21x21 grid corresponding to the detector pixels. We sample, all 480 fibres on one half of the slit and trace 10^6 rays for each attempt to obtain PSF values. Then, we use cubic splines to fit the PSF intensity and position for each fibre over the full wavelength range and convolve this with high resolution input spectra scaled to the desired target magnitude. Detector noise and sky background (emission and absorption) are added, and the final spectrum for each object is inserted into the data frame.

Now we can establish the data sets as a result of this Zemax simulation by using 480 data points for 9 wavelengths for 5 configurations, i.e. 5*9*480=21600. The data from Zemax ray tracing are then ingested into a Python code one fibre at one time. For each fibre, we stack the 9 PSFs into a 3 dimensional array, and then apply a spline interpolation along the wavelength direction for each pixel in the 21x21 image grid.

3.3.1 Basic concept of interpolation for the PSF

The basic concept of this procedure, i.e. interpolation between grid data sets, is getting new flux data sets at new wavelengths/pixel positions between the given wavelengths and positions from the Zemax ray tracing simulation. However, the concept of linear interpolation in the code is more complicated because the Zemax PSFs are encoded as pixel grids centered on the peak of each PSF, not on the actual (non-integer) CCD pixel coordinates of the location of that PSF. This is shown in Equation 6 and Figure 23: (x_1, y_1) and (x_2, y_2) are not assumed to be in a common CCD frame, but represent a property of each PSF. In fact, y_b is wavelength and x_a is the spatial coordinate that we want to get from the interpolation function. U_1 and U_2 are the intensity distributions, and W_1 and W_2 are assumed to be the monochromatic wavelength of each PSF.

$$\left(\frac{y_2-y_1}{x_2-x_1}\right)x_a+\frac{y_1x_2-x_1y_2}{x_2-x_1}=y_b \qquad (6)$$

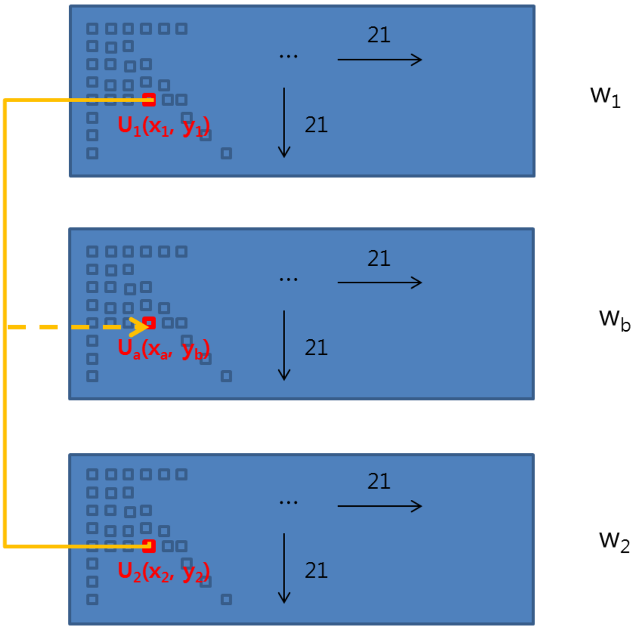

Figure 23 Diagram for the general concept of interpolation between PSF and wavelength. The calculation method currently has been changed, however the concept still can be explained how the interpolation is working in the simulator. It seems to interpolate between the wavelength, W_1 and W_2, and PSF, U_1 and U_2, but infect the PSF values consist 2D array. According to equation 6, y_b is interpolated value at x_a but in this case $U_a(x_a,y_b)$ is actual interpolated value at the wavelength W_b between W_1 and W_2.

3.3.2 Position correction using footprint data

Based on this concept, we can get the interpolated intensity for each wavelength and pixel position from a subroutine in the simulator. We also have to think about footprint data from Zemax simulation, because the PSFs pixel coordinates are not directly mapped to the CCD pixels. As shown the Figures 13, 14, 15, 16, and 17 in the previous chapter, the PSFs maps from Zemax are not fixed in the centre along the given wavelengths, fields, and other configurations. Therefore, we need to calibrate the relative position for each other and correct it before interpolating the data. This procedure is shown below and in Figure 24, and we can calculate each area from 1 to 4 using the lengths a, b, c, d when we assume the side of the whole area equals 1.

$$\text{Area 1} = a \times c$$

$$\text{Area 2} = b \times c = (1 - a) \times c$$

$$\text{Area 3} = a \times d = a \times (1 - c)$$

$$\text{Area 4} = b \times d = (1 - a) \times (1 - c) = 1 - a - c + ac$$

The calculation presented in the subroutine of the simulator.

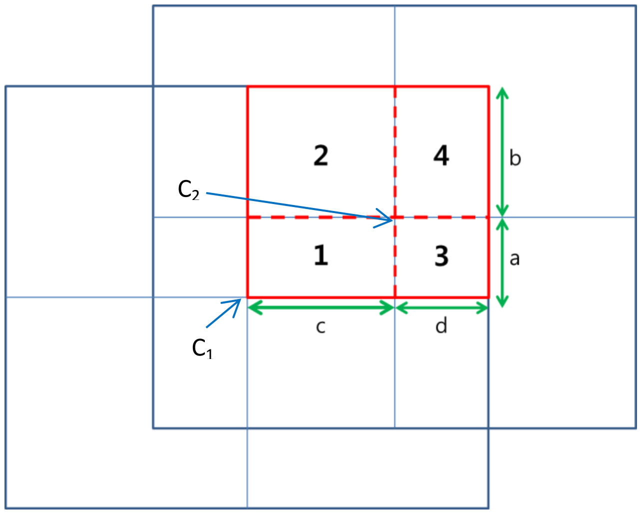

Figure 24 Basic concept of interpolating PSF using footprint data. The result images from each simulation in Zemax are not fixed on the specific point, we can calculate the decenter value from footprint data and correct the relative position of PSFs. C_1 is the fixed center of PSF values for every 21 X 21 grid before calibration, and we can get new C_2 from footprint data. So the sum of each area 1, 2, 3 and 4 (red box) means the new PSF area after calibration of the center from C_1 to C_2.

3.4 Development of the WEAVE image simulator

3.4.1. Spectral libraries for the simulator

We now sample this spline over 20,000 points and have an array in the wavelength direction. For each fibre, we randomly assign a spectral template and scale to an appropriate input magnitude. We can find several stellar spectral samples from online libraries to provide input spectra for a simulation, and to divide the libraries into empirical and theoretical catalogues based on the method of getting data [Chen et al., 2014].

Generally, we gather a collection of stellar spectra that is classified by similar range of wavelengths and resolution, effective temperature (T_{eff}), surface gravity (log *g*), metallicity ([Fe/H]), and spectral information for a broad range of wavelengths are required as the elements can make changes to the stellar spectra.

As shown in Table 8 and 9, the popular spectra libraries are Coelho et al. (2005), Coelho et al. (2007), Allard et al. (2011), and Palacios et al. (2010) for theoretical libraries, and the advantage of the libraries is that the objects and the stellar spectra can be generated with arbitrary parameters such as resolution and metal abundance. On the other hand, the empirical libraries had a limitation previously for selecting the target object because it was based on real observation with telescopes. However, many innovative studies of spectra library have been produced by e.g Lançon & Wood (2000), Lançon and Mouhcine (2002) and Rayner et al. (2009).

Table 8 List of empirical libraries

	Name of Library/Objects	Wavelength coverage (nm)	Resolving power (R)	Number of stars	Reference
Empirical libraries	ELODIE	390-680	10000	1388	Prugniel and Soubiran (2001, 2004)
	Stellar spectral flux library	115-1062, ~ 2500		131	Pickles (1998)
	IUE Atlas	115.3-320.1	500	229	Heck et al. (1984)
	EUVE stellar spectral Atlas	7-19 (SW) 14-38 (MW) 28-76 (LW)		95	Craig et al. (1997)
	H-Band Spectra	H band	3000	85	Meyer et al. (1998)
	Lick/IDS	400-640	8-10Å	455	Worthey and Ottaviani (1997)
	MILES	2000	352-750	985	Sánchez-Blázquez et al. (2006)

Table 9 List of theoretical libraries

	Name of Library/ Objects	Wavelength coverage (nm)	Metallicity ([Fe/H])	Teff (K)	Reference
Theoretical libraries	Stellar spectra with scaled-solar and α-enhanced mixtures	300-1340	-0.5, 0.0 and 0.2	3000-25000	Coelho et al. (2005, 2007 and 2014)
	Pollux (O and M stars)	300-1200	0.0		Palacios et al. (2010)
	VLMs (Very Low Mass Stars), BDs (Brown Dwarfs)		-1.5, 0.5	400-100000	Allard et al. (2011)

For the low-resolution spectra of WEAVE image processing simulation, the templates we have initially adopted are taken from the X-Shooter Spectral Library (XSL) produced by Chen et al. (2014). This library contained 237 stars with wavelengths between 3000-10200Å, the resolution, R =λ/Δλ, is 10000 and O-M, C, and S stars are listed on the library, which has been obtained from VLT (Very Large Telescope) at Cerro Paranal, Chile. XSL has a merit, compared with the other libraries, because the wavelength coverage is broad and the stellar spectra are obtained at higher resolution than WEAVE.

For the high-resolution modes, we use synthetic spectra that were generated for the 4MOST project by Caffau et al. (2012) as shown in Figure 25. The 4MOST is a 4m Multi-Object Spectroscopic Telescope at the VISTA (Visible and Infrared Survey Telescope for Astronomy) with a very wide FOV (Field of View) ~3 deg^2 and a fibre-fed spectrograph similar to WEAVE, albeit in the Southern Hemisphere. The requirements for simulated spectra are determined for the general class of Galactic targets. For example, the values of effective temperature (T_{eff}) for dwarfs are 6500K and 5500K, and the T_{eff} for giants is 4500K. The surface gravity (log *g*) is selected to be 3.0 and 4.0, and metallicities ([M/H]) are determined as +0.5, 0.0, -0.1, -0.2, and -0.3 for dwarfs and 2.0 and 1.0 for giants.

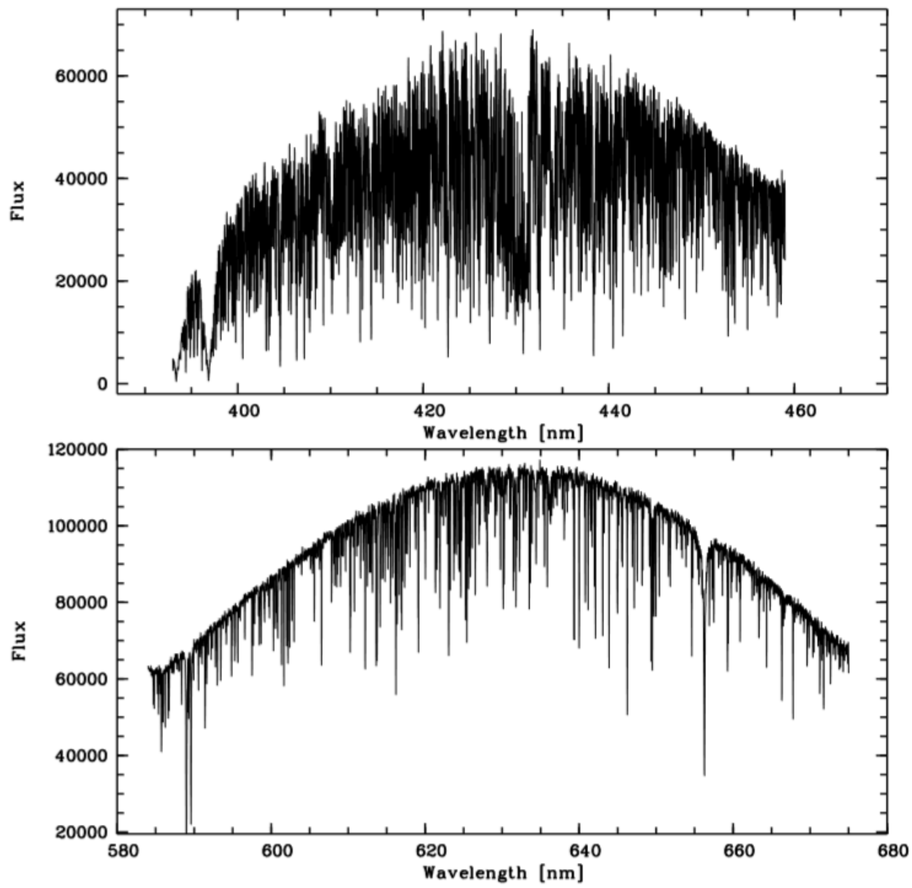

Figure 25 Simulated spectra from Caffau et al. (2013). The star is selected with parameters effective temperature (T_{eff}) = 5500K, surface gravity (Log *g*) = 4.0, and metallicity ([M/H]) =0.0 at r = 14mag. Upper spectra for the blue arm and the bottom is for red arm.

3.4.2 Sky Model

The next phase of the development of an image simulator is to adopt a suitable model for the sky background. For this calculation, there are several atmospheric radiative transfer codes, such as MODTRAN (Berk et al., 1998), LEEDR (Fiorino et al., 2014), COART (Jin et al., 2006), and HITRAN (Rothman et al., 2013). In this case, the COART model is much more related with aspects between atmosphere and sea surface and LEEDR is US government software that is difficult to use although it is a powerful tool in terms of extended solar and lunar sources, including single and multiple scattering. MODTRAN and HITRAN is quite useful and popular code for calculating atmospheric effects including radiance, scattering, and polarization.

Sky spectra for each input template has been taken from the ESO SkyCalc and the Sky Model Calculator by Noll et al. (2012). SkyCalc is an application based on the Cerro Paranal Advanced Sky Model. This model has two parts, called 'modules': the first module calculates synthetic sky background spectra using the data from radiative transfer code, HITRAN 2008. Advanced model HITRAN 2012 now has 7,400,447 spectral lines for 47 different molecules. [Rothman et al., 2012] The second module of Cerro Paranal Advanced Sky Model contains additional components for sky background such as scattered moonlight, scattered starlight, zodiacal light, telescope emission, and atmospheric emission [Noll et al., 2013].

We provided from ESO SkyCals the broad-band magnitude, Airmass, scattered moonlight along the moon phase from 0˚ to 360˚, while other scattering effects from the atmosphere and emission line as explained above. The information of sky background calculation is included in the simulator header.

3.5 The WEAVE image simulator

We call the simulator for WEAVE image processing and spectral extraction as WEAVESIM, running under Python.

The main procedure of the WEAVE simulator is shown in Figure 26. First, number 1 is basically used for declaring all commands and directories for using data sets. Also, it concludes the mode that we want to change to calculate between blue (mode 1, 2, and 3) and red (mode 4 and 5) wavelengths and high (mode 2 with high resolution band 1 and 3 with high resolution band 2, and mode 5) and low (mode 1 and 4) resolutions. Then from number 2, subroutine 'set_mode' and the other part uses pre-setting/calculating the main interpolation for PSFs and wavelengths. Then from number 15 to 18, 26, 28 to 31, and 45 are used for reading data into the simulator to calculate the values for spectral extraction such as sky value and target stars. For the sky values, it now contains general information of the transmission of atmosphere and scattered light from any related surface according to Moon phase change and telluric bands.

The subroutines from 15 to 17 involve the data acquisition of PSFs and footprint data that is the position on the detector from the previous simulation using Zemax. Afterwards, we can use these data to get the result of the flux at interpolated wavelengths/positions. As a result, we can use all data to produce various plots, which are presented from subroutines 35 to 41 and 57 and 58. The other parts are for writing/making FITS file and its header. The header of FITS file can be changed to add more lists in the future.

- Specifying the initial values: declaration of each command and directories for the steps of several calculations inside of the code. Here the code can determine which mode (low and high resolution for each blue and red wavelength) will be used for the calculating PSFs and extracting spectra. The data about the sky from SkyCalc are added recently, so they are assumed as airmass = 1 and extinct = 0;
- set_mode: declaration the name/directories of each file and calling each file from Zemax PSFs and footprint data. Setting sky mode between bright (full moon) and dark (new moon) sky. Setting throughput data and arc for each mode;
- fibre_to_spectrum/spectrum_to_fibre: the number between fibre and spectrum is

converted in the code. There are fibre numbers that do not exist on plate A, so we need to check carefully when the numbers are selected during running the simulator;

- input_field: As the fibres can move during the observation by position, this term determines the position, angle, and vignetting factor when the fibres are moving on the plate;
- pri_vignette: it returns the vignetting at the telescope focal plane as a function of field angle in degrees;
- ntc_vignette: it returns the vignetting in the spectrograph if input telecentricity is mis-aligned. Input is in radians;
- bias_gen : generate bias with random number generator;
- add_noise: generate noise value with Poisson distribution and return np.random.poisson;
- shift_chips: shift and make a gap between two chips and return last_pix1y andfirst_pix2y; As the WEAVE optical design has been changed, the image plane is divided with two individual chips and there is a gap between the chips. So this function produces the gap in the simulator.
- spline_fit: spline interpolation fitting and return out;
- gen_sky2: generate sky value and sky transmission from gen_sky3(generate sky value and sky transmission from ESO SkyCalc application), then make it linear in pixel coordinate and return scale4, sky4, skyn, and skt4. The other term of generating sky is ‘gen_sky’ , derive the value from the Xshooter sky files;
- spec_in: fits file header for spectrum;

- get_spec: make spectrum file, return specn. If the mode is 4, sp3 (spectrum of mode 4) matches the spectrum to the sky basis. The noise is added now, which is normalized to photons/pixel assuming 100% throughput in 1 hour exposure at WHT;
- map_psf: mapping specific psf for any particular fibre;
- add_fibre2: Rectbivariate interpolation is a Bivariate spline approximation over a rectangular mesh, and we calculate I(x,y) with given footprint data, which is faster than the add_fibre routine because we now do one flat and two arcs. We changed the multiplication of the PSF by spectot (in write_target()) to pass in the three spectra to add_fibre() and then only evaluate each spline fitting once instead of three times and use intp.RectBivariateSpline();
- fitsprimary: generate fits header and return hdu0. It contains a great deal of information about target, time required to observe the status and condition and detect the target;
- fitstable: generate a table of fits header and return table HDU;
- posfitstable: generate a table from the targ_array data. It contains information such as magnitude (r, i, g, v mag), target number, position and fibre number.
- combine_sky: obtain the best estimate of the spectrum for the image, and make the final sky spectrum, which is subtracted from the target spectra. It takes a median of the data in all the sky fibres, but applies the appropriate normalization factors to remove the effect of the vignetting differences;
- sky_subtract: subtract sky value from the data using extract_fibre;
- extract_fibre: extract data from one single fibre;

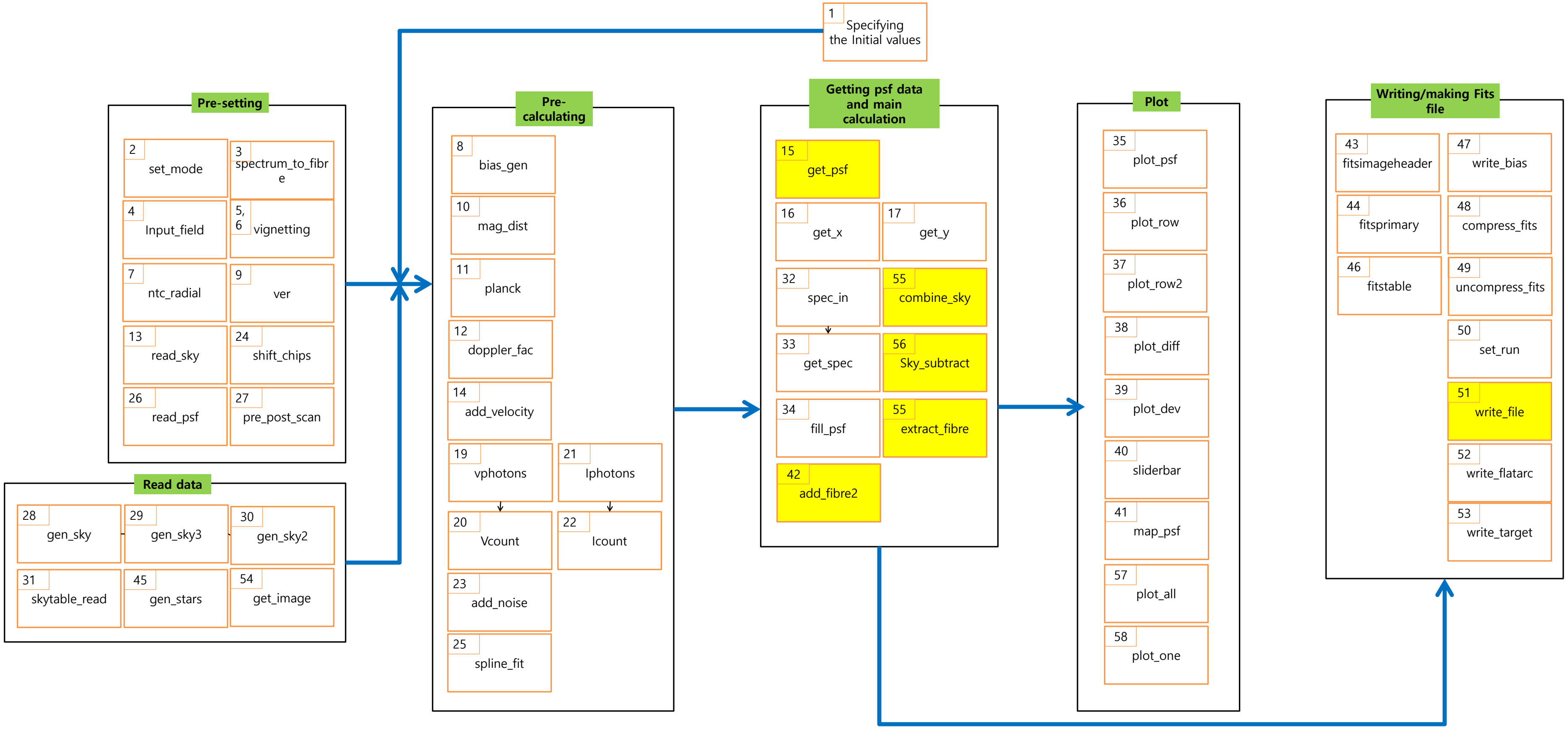

Figure 26 WEAVESIM data flow. WEAVESIM is the simulator for WEAVE image processing and spectral extraction. There are six individual parts, and the information and fixed setting/calculated data/scientific constants in the 'pre-setting' part pass to pre-calculate the simulator. That is included in calculating the magnitude, Doppler Effect, bias, and flat etc. As the input data size for the simulator is quite large, there is the individual 'read-data' part. This is for on-line acquisition data such as sky value from SkyCalc and others for getting data such as fits files. 'The getting PSF data and main calculation' part is the most important, and all of main calculations include components such as combine_sky, add_fibre1, and extract_fibre. The 'plot' part contains general codes for any plot for useful setting, and the last part, 'writing/making fits file', is for getting and storing the data as a fits file and compressing the data to a reduced size. Additionally, this part contains a header, which provides useful information for users in the future.

Chapter 4

Spectral Extraction of Simulated Data

4.1 Introduction

We show the results of the WEAVE simulator and describe the progress in this chapter. Developing a simulator to verify the performance of the optical/whole system is one of important procedure during the project, therefore we can meet the result of the project – developed spectrograph and its data for the community, and the goal – science objects finally.

In the previous studies about a simulator for other projects, they use different, various software to develop their own program. The HERMES (High Efficiency and Resolution Multi-Element Spectrograph) instrument among them has similar tool with WEAVE simulator [Goodwin et al., 2010]. This instrument had been planned for the Anglo-Australian Telescope to study Galactic archaeology; it has high resolution (R~50000) multi-object fibre-fed (392 science fibres) spectrograph with VPH grating like WEAVE. The end-to-end instrument data simulator developed using MATLAB and the optical information passed from Zemax, the name of the simulator is HERMES Data Simulator (HDS). The benefits and advantages of developing this simulator are [Math works, 2010];

- innovation : improve efficiency using common design environment and possible fast design trade-offs
- quality : possible testing to identify and correct errors with linking designs directly to requirements
- cost : develop cost effective model instead of physical prototypes and testing, reusing test suits
- time : reduce error and find correct procedure after starting mission

The differences of the simulator between WEAVESIM and HDS are not only for the developing software, but also using data sets from Zemax. HDS took geometrical images aberration, but made grid 11 x 10 and interpolated by cubic polynomials for all 400 fibres. The simulated detector images (flat, arc and object fields) for the HERMES blue band (R ~ 30000, wavelength ~ 475nm) are shown in Figure 27, the sample images for WEAVESIM are shown in Figure 28 below.

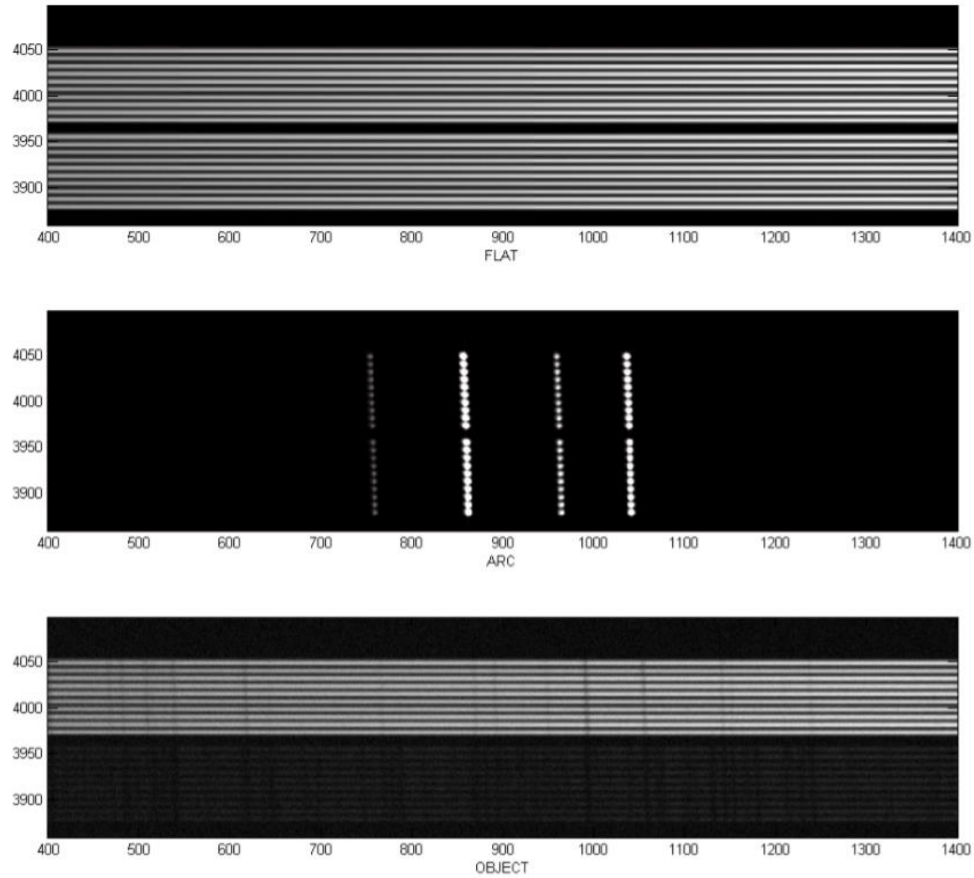

Figure 27 HERMES simulated detector images, from top to bottom, flat, arc and object fields. It covers from fibre 381 to 400 only. [Goodwin et al., 2010]

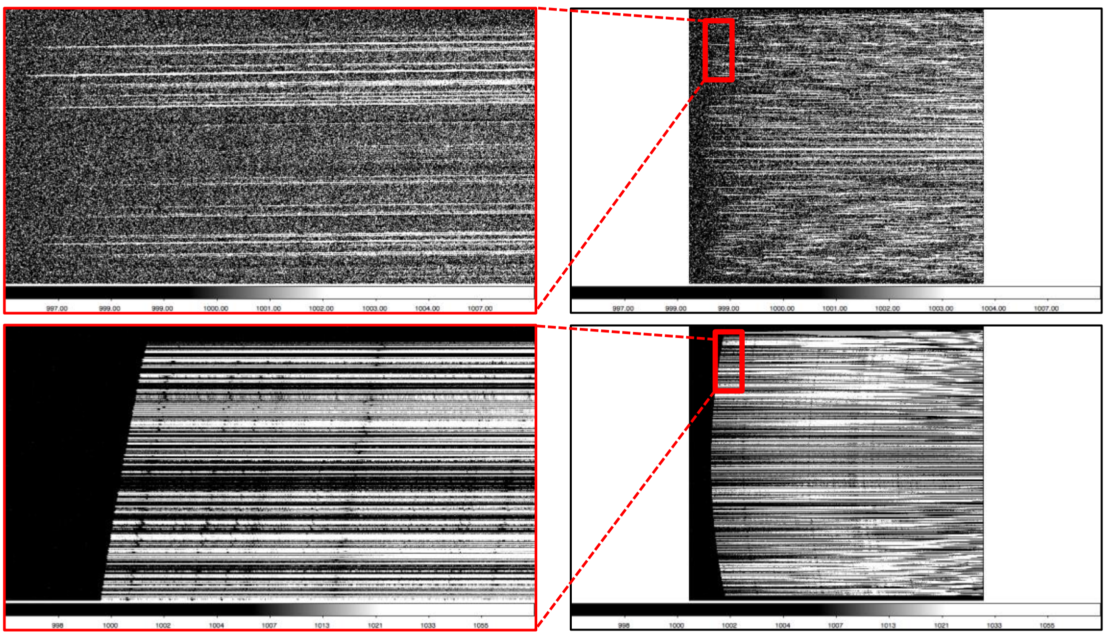

Figure 28 The result images of the whole size 6k*6k from WEAVE simulator. (top pair) Low resolution in blue band STePs sample image. (bottom pair) High resolution in blue band halo field sample images.

The new data sets of PSF can be taken for each wavelength; the whole PSF sets from the simulator are shown in Figures 29-33. These are matching with Figures 13-17, the PSF sets from Zemax simulation. We found some pattern in this figure earlier, it shifted to vertical direction for every 3~4 points in different wavelength and questionable if this was related with ripples in regenerated spectral images. However we checked this problem again and now we think this is from miscalculation of interpolation. We had too high an order of spline fitting for x and y positions of the each PSF, if we once changed the order of polynomials then the pattern was removed.

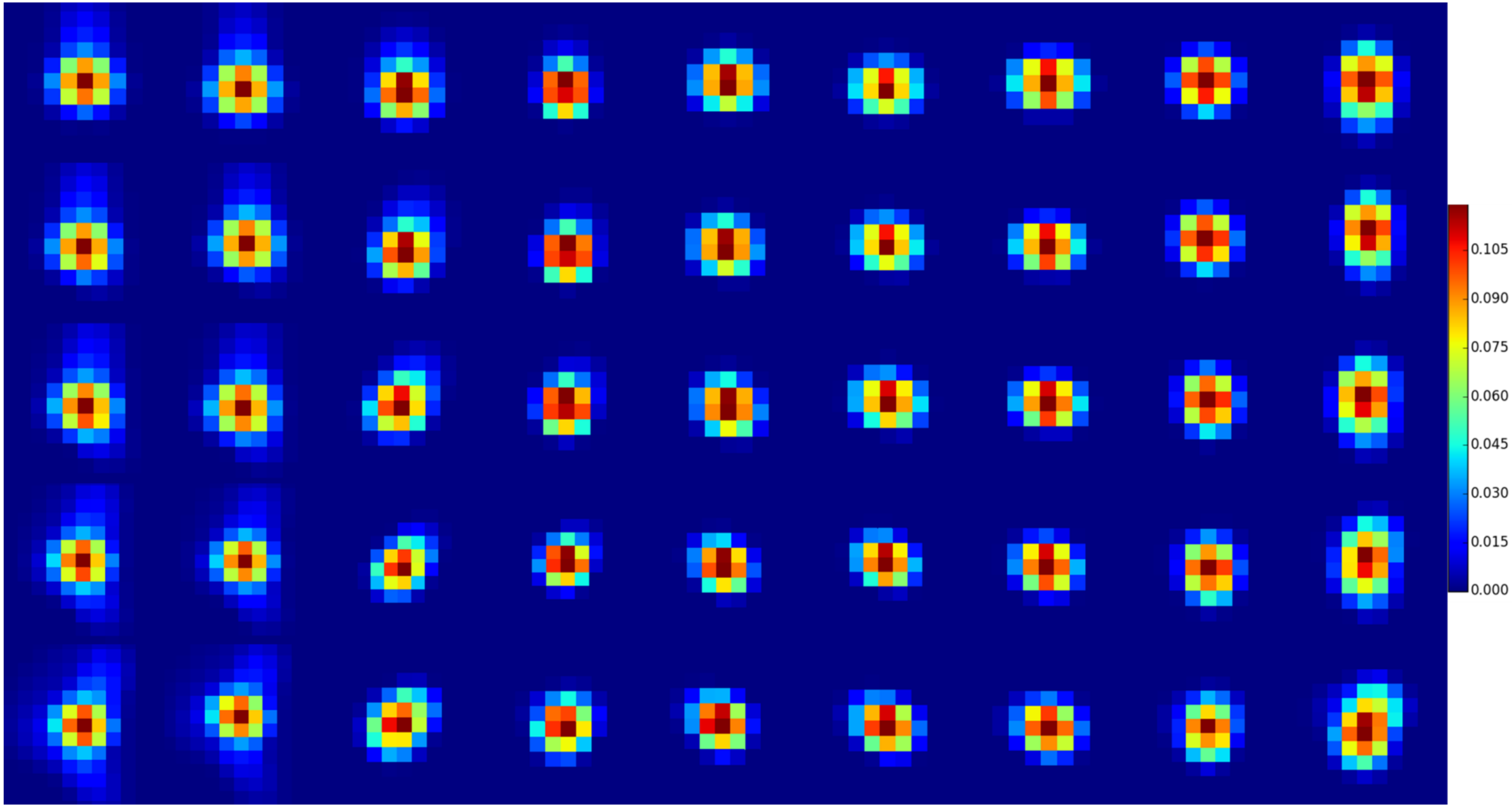

Figure 29 The PSF images of the focal plane from PSFs from WEAVESIM simulator. These images are for configurations 1 of 5. From the first row, fibre number=1, 120, 240, 360 and 479. The 9 wavelengths are from 0.3660μm to 0.6060μm of configuration 1.

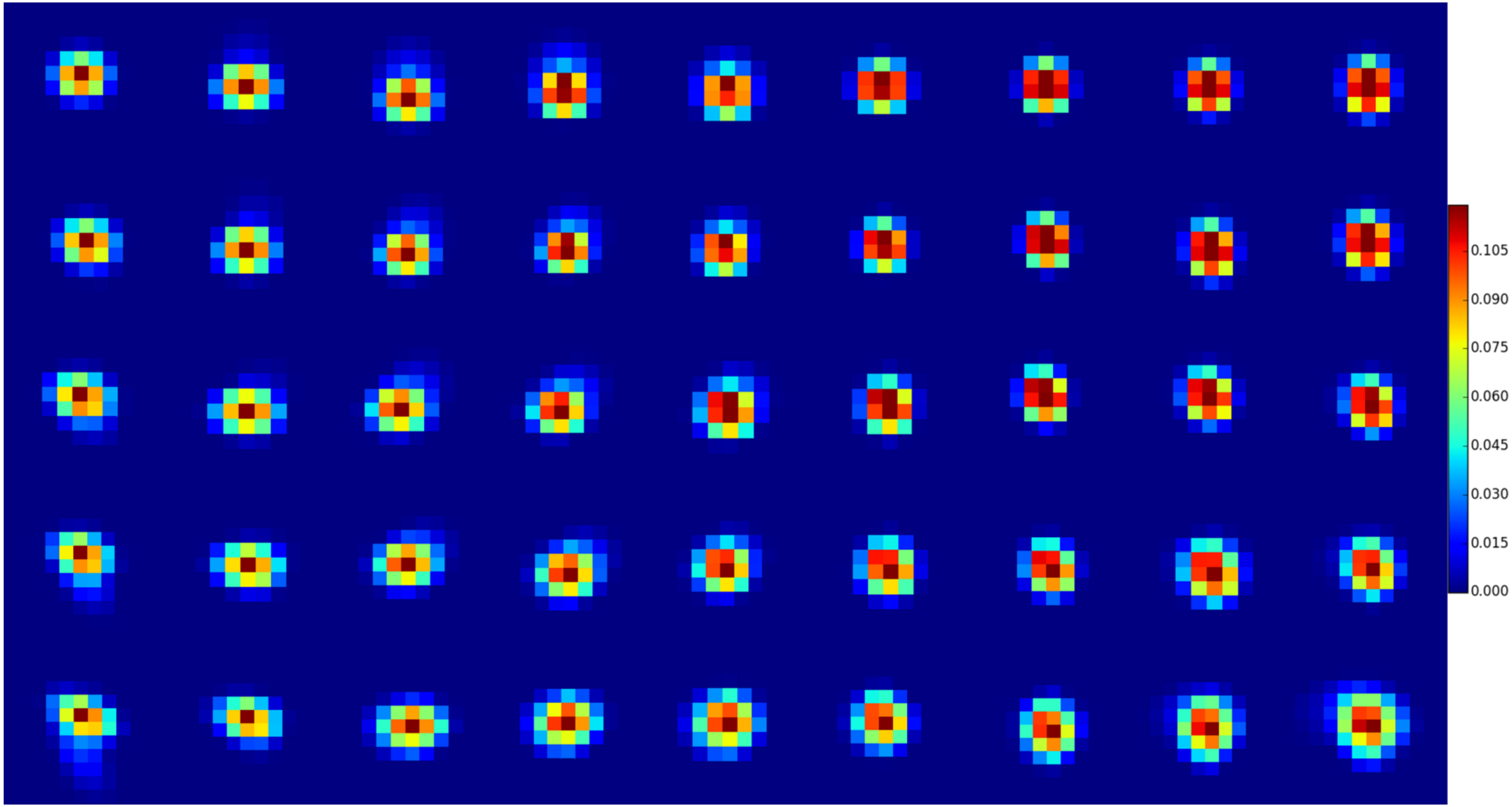

Figure 30 The PSF images of the focal plane from PSFs from WEAVESIM simulator. These images are for configurations 2 of 5. From the first row, fibre number=1, 120, 240, 360 and 479. The 9 wavelengths are from 0.4040μm to 0.4650μm of configuration 2.

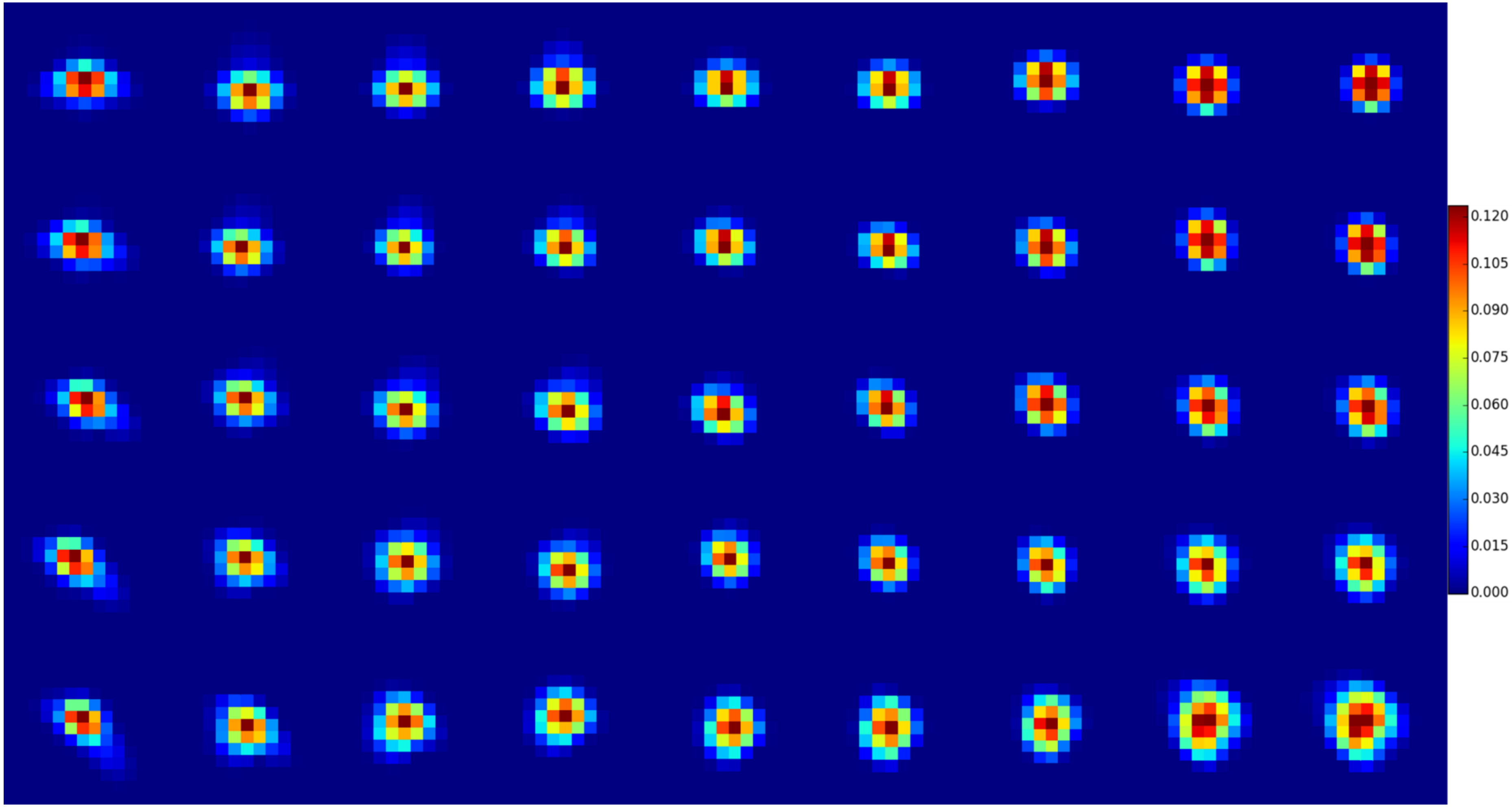

Figure 31 The PSF images of the focal plane from PSFs from WEAVESIM simulator. These images are for configurations 3 of 5. From the first row, fibre number=1, 120, 240, 360 and 479. The 9 wavelengths are from 0.4730μm to 0.5450μm of configuration 3.

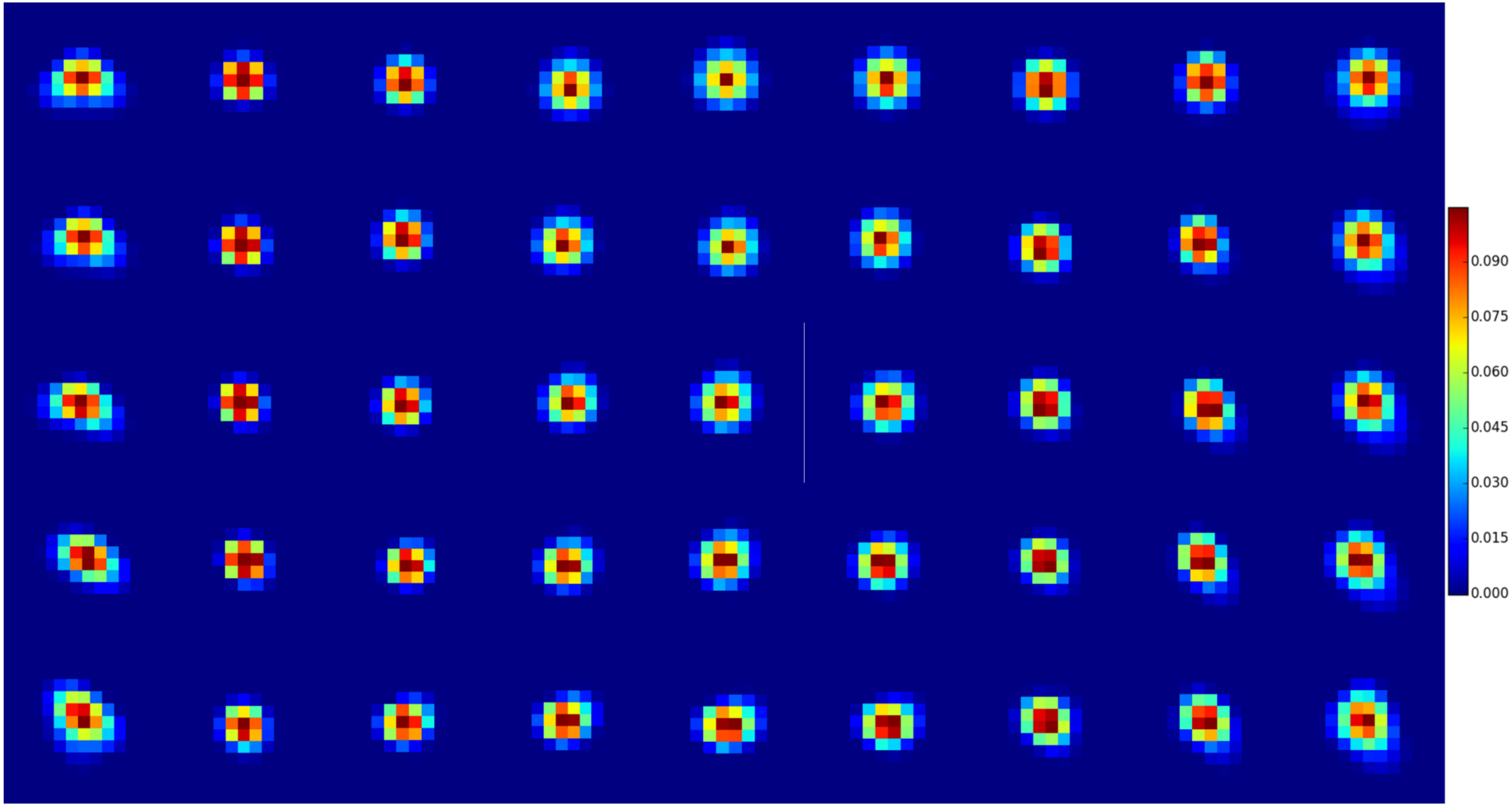

Figure 32 The PSF images of the focal plane from PSFs from WEAVESIM simulator. These images are for configurations 4 of 5. From the first row, fibre number=1, 120, 240, 360 and 479. The 9 wavelengths are from 0.5790µm to 0.9590µm of configuration 4.

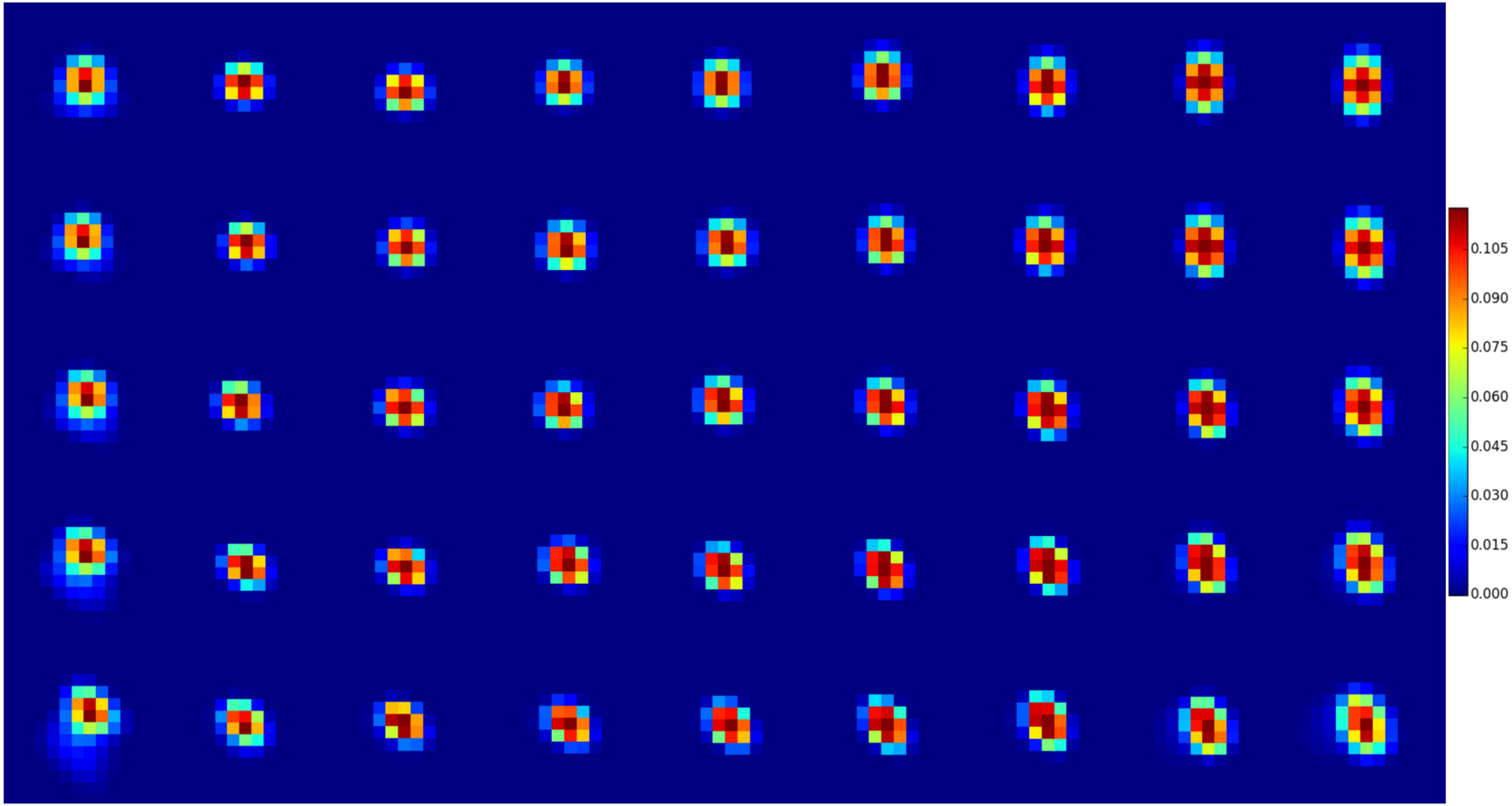

Figure 33 The PSF images of the focal plane from PSFs from WEAVESIM simulator. These images are for configurations 5 of 5. From the first row, fibre number=1, 120, 240, 360 and 479. The 9 wavelengths are from 0.5950μm to 0.6850μm of configuration 5.

Sample template and output spectra for the high-resolution mode are shown in Figure 34 as below. These simulated spectra from WEAVESIM previously, i.e. earlier model in 2015. Simulated image of bottom in the figure is a part of the spectra from top image, these are not exactly generated from the original sample spectra.

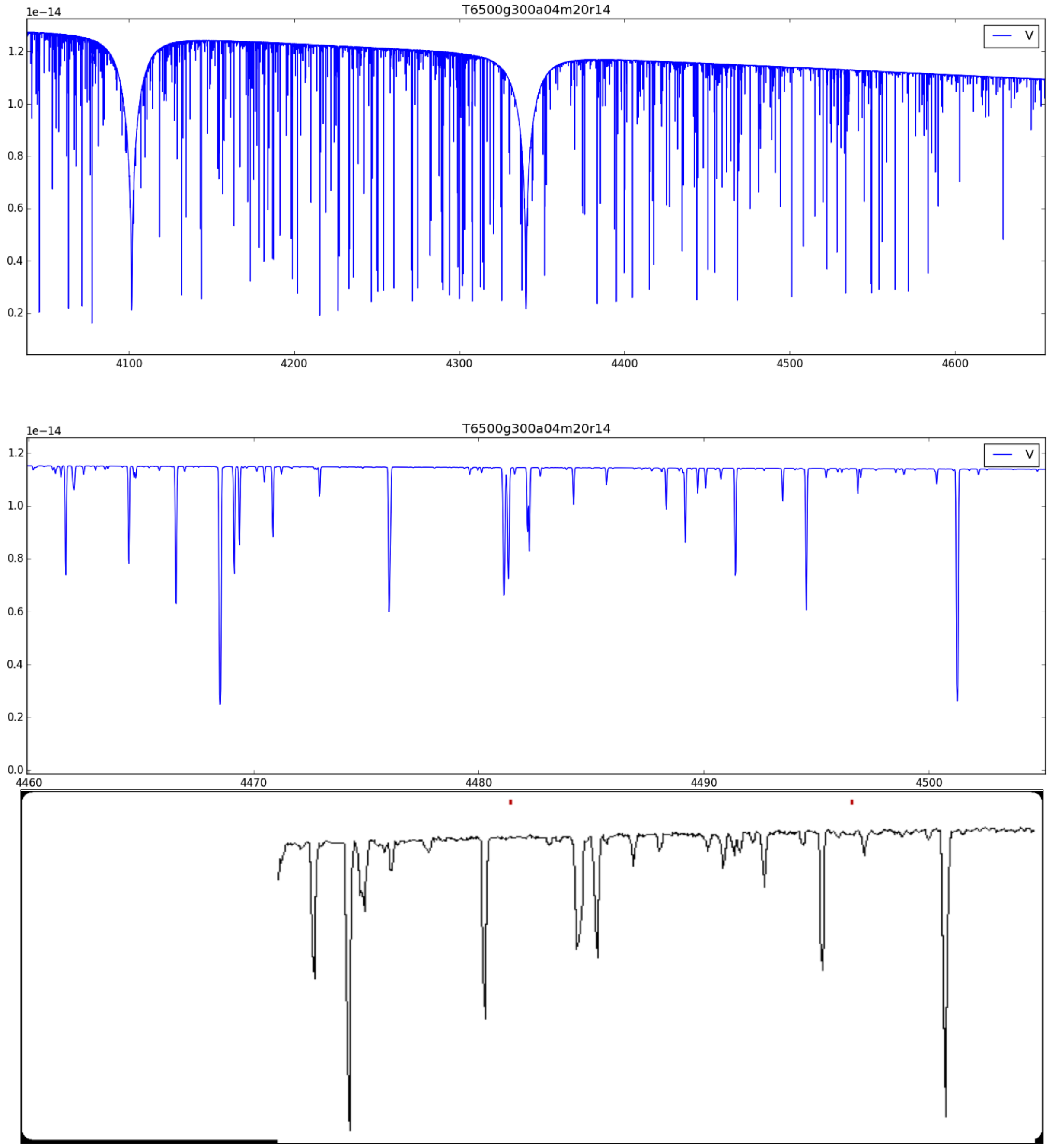

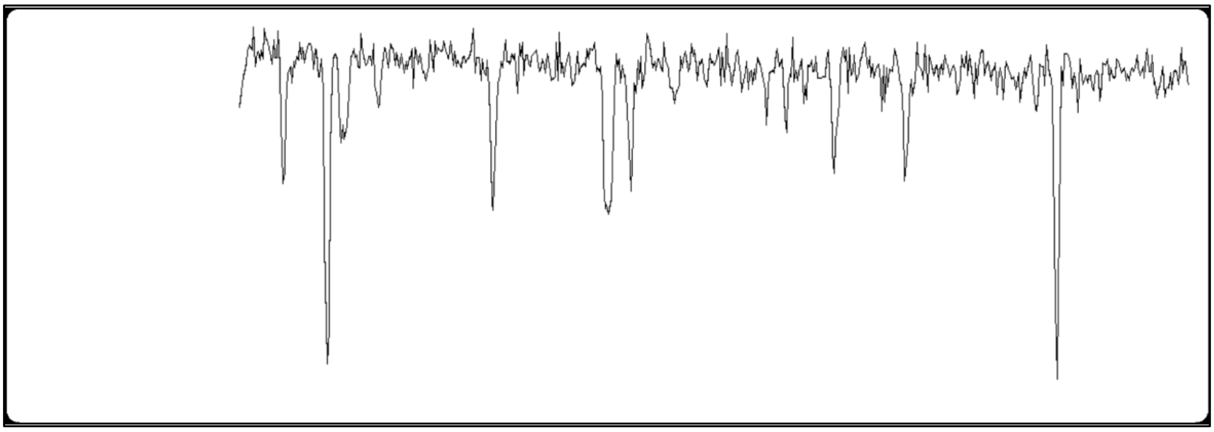

Figure 34 Top panel is typical input blue spectra from the high-resolution library. Second panel Zoom in on a detailed subsection of the input spectrum from top image and third panel is the recovered 1-D sky subtracted spectrum for V=12, the last panel is the same object recovered from an input fibre with V=16.5

4.2 Simulated Observing Run

After extensive development of the simulator, then the spectra have been regenerated recently, and a full set of simulated data generated for initial evaluation by CASU. The template images consist of three sets as below;

- Total 7 hours exposures of Low resolution data for STePS (Stellar Populations at Intermediate Redshifts survey) in Red and Blue wavelength. The STePS project is for analyzing stellar populations and galaxy evolution. 7 sets of Elliptical galaxies at z=0.4, z=0.6 and z=0.9 each is one set of template and exposures for 20min each. (3 group for each different redshift x 20min x 7 sets = 7 hours total exposure)

- Total 1 hour observation (3 frames each) of a simulated halo field with some stars from XSL and some LOFAR-like galaxies from Kinney and Calzetti [Kinney et al., 1996; Calzetti et al., 1994].

- Total 2 hour observation of a simulated HR stellar field using spectra from Caffau et al., 6 frames each for Blue and Red wavelengths, 2 hours exposure total.

4.3 Sky Spectra

The result input sky spectra into WEAVESIM are shown below. The x axis represents the wavelength for each configuration and y axis is energy flux with arbitrary unit. The results shows the WEAVESIM simulator works properly with all template data we applied, the regenerated images are compared with the template image in each step.

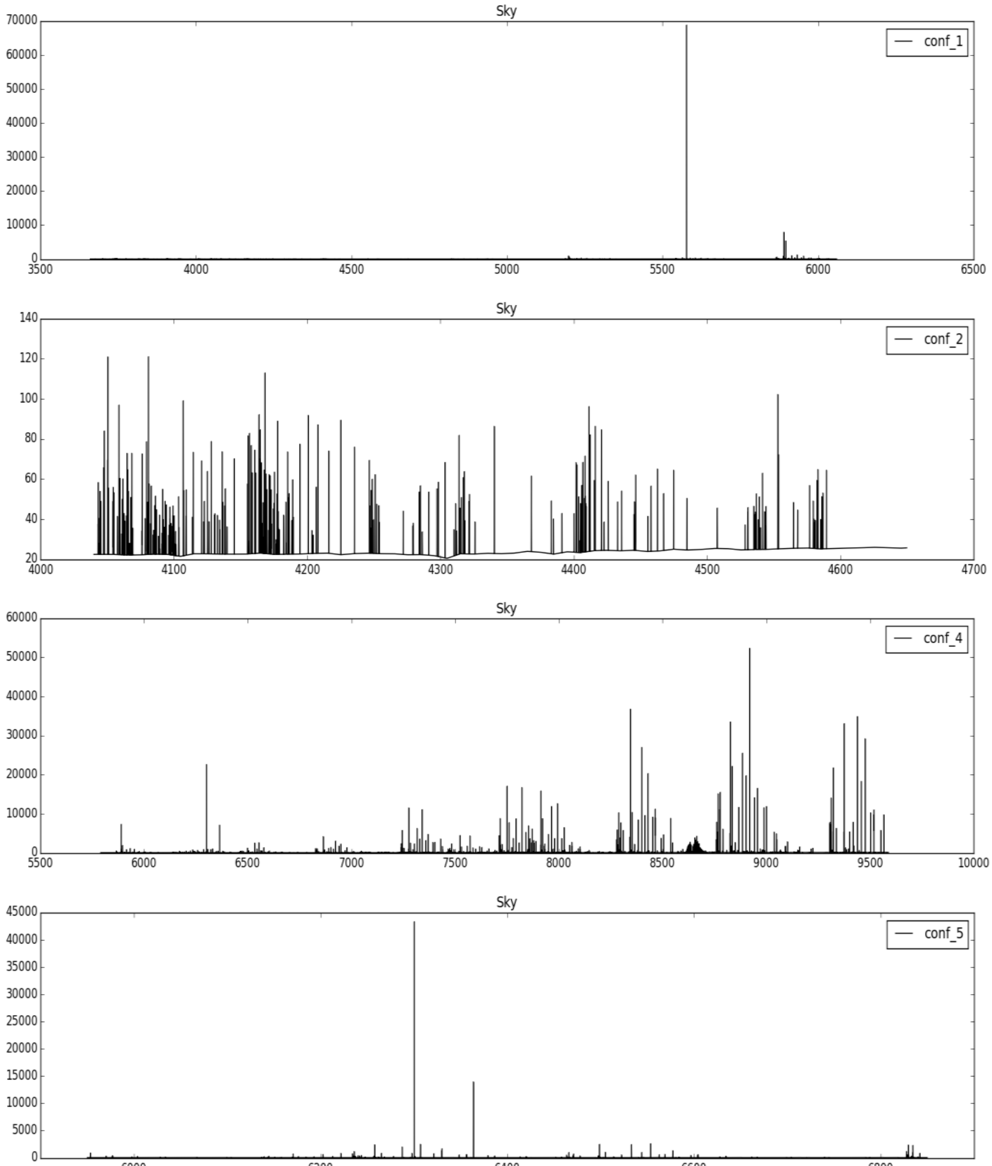

Figure 35 These regenerated spectra are the input sky returned by gen_sky2(). The values are calculated from ESO SkyCalc. From the top to bottom is mode 1 (Low resolution for blue band), mode 2 (High resolution for blue band), mode 4 (LR for red band) and mode 5 (HR for red band).

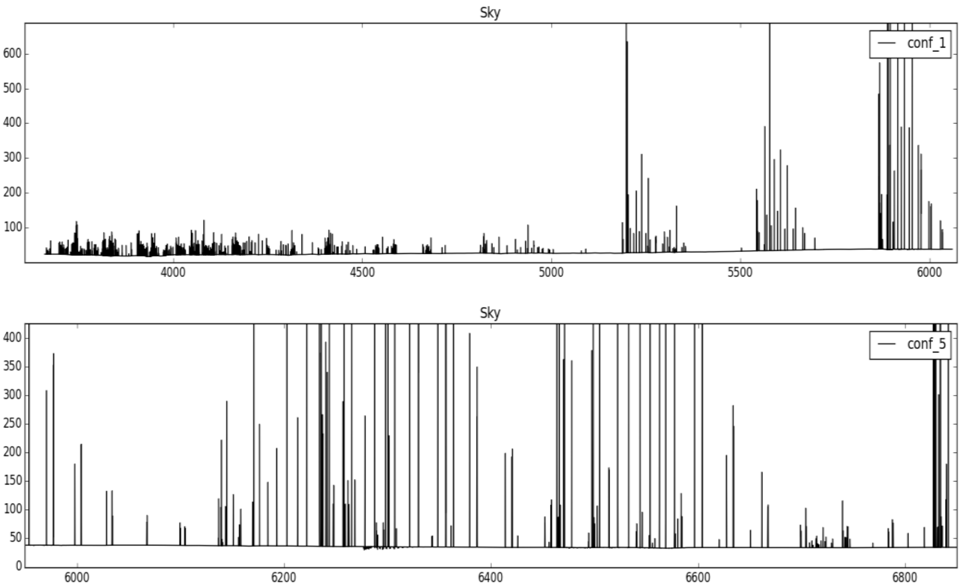

Figure 36 These are a part of the input sky spectra for mode 1 and mode 5, zoomed in the flux scale.

The Figures 37 and 38 show simulated spectra of the Low resolution mode in the blue and red wavelength band from STePS template images. Each image is 20mins exposure, so we combined 3 images for generating 1 hour exposure template images.

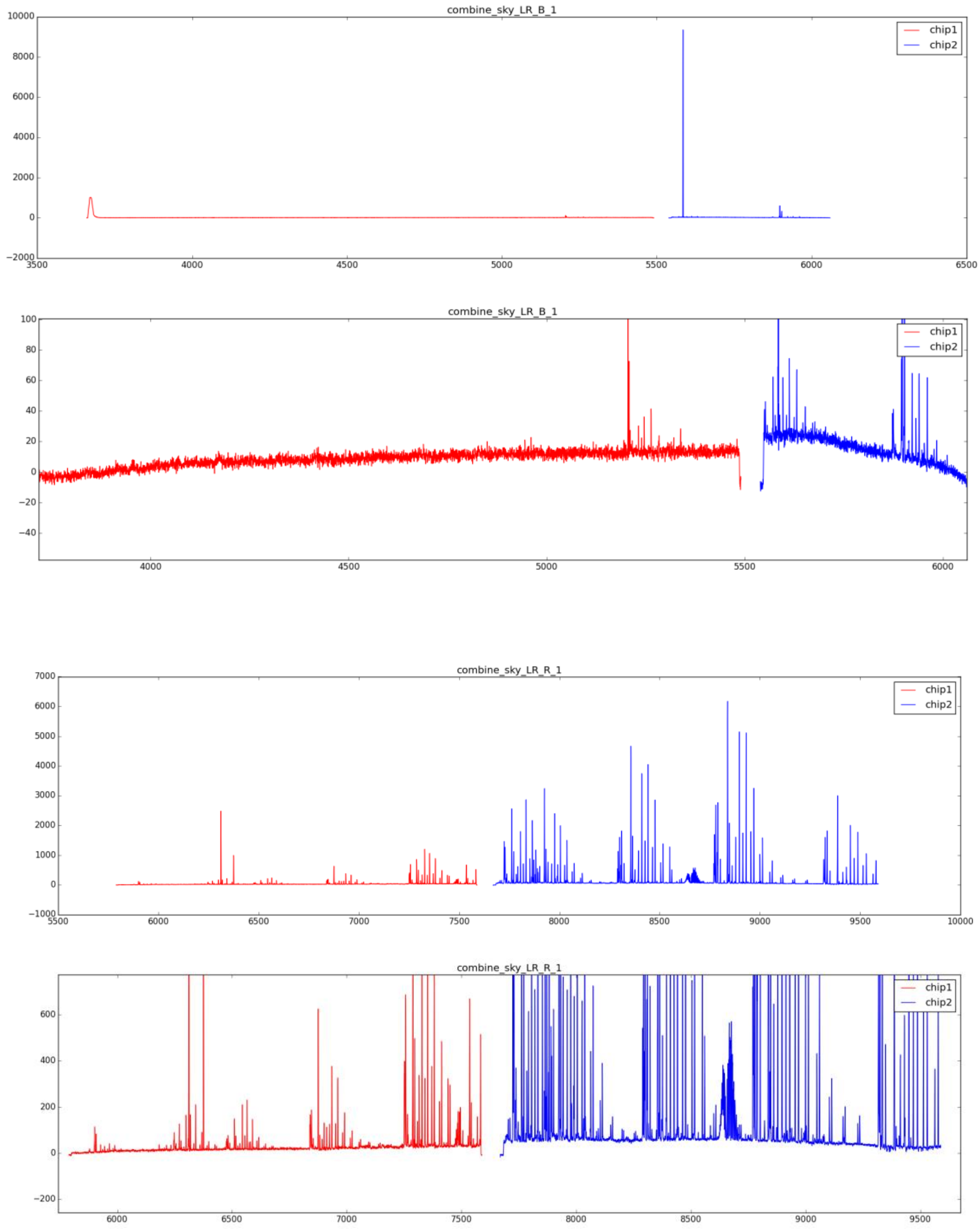

Figure 37 Simulated images from 1 hour of STePS data for Low resolution mode. Top pair: final blue combined sky spectra from the 44 targeted sky spectra. The lower image is zoomed in from first image to reveal the continuum. Bottom pair: same for the red arm data. The combination takes median of the data in all sky fibres, using the appropriate nomalisation factors applied to remove the effect of the vignetting differences, so this has noise properties closer to what we will get in reality.

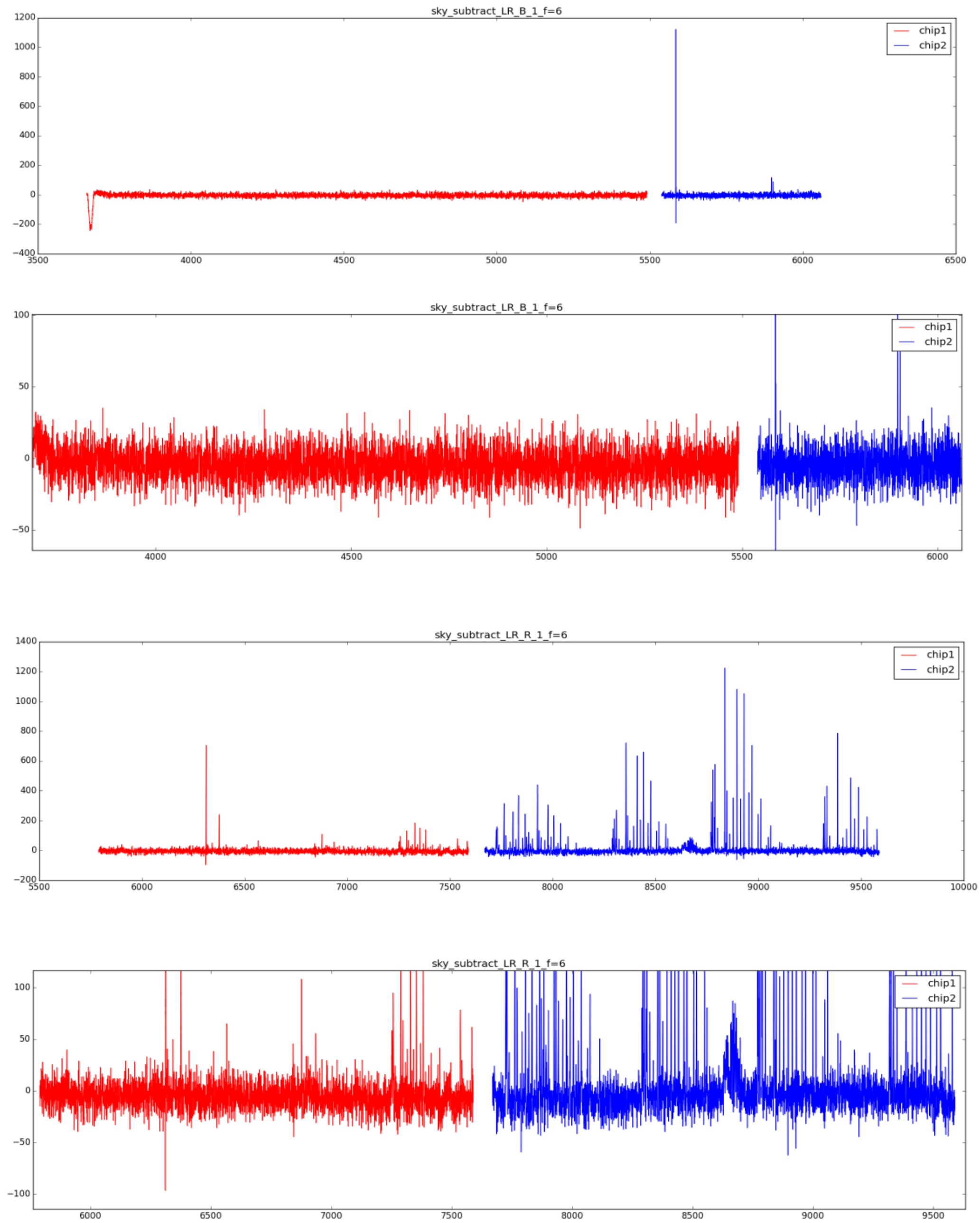

Figure 38 These images are the sky spectrum for a single fibre for a 1 hour exposure after the mean combined sky fibre has been subtracted with the appropriate scaling factors. Top pair: Blue spectra and zoom; Bottom pair: Red spectra and zoom. The residuals from the noise in the sky spectra are clearly apparent.

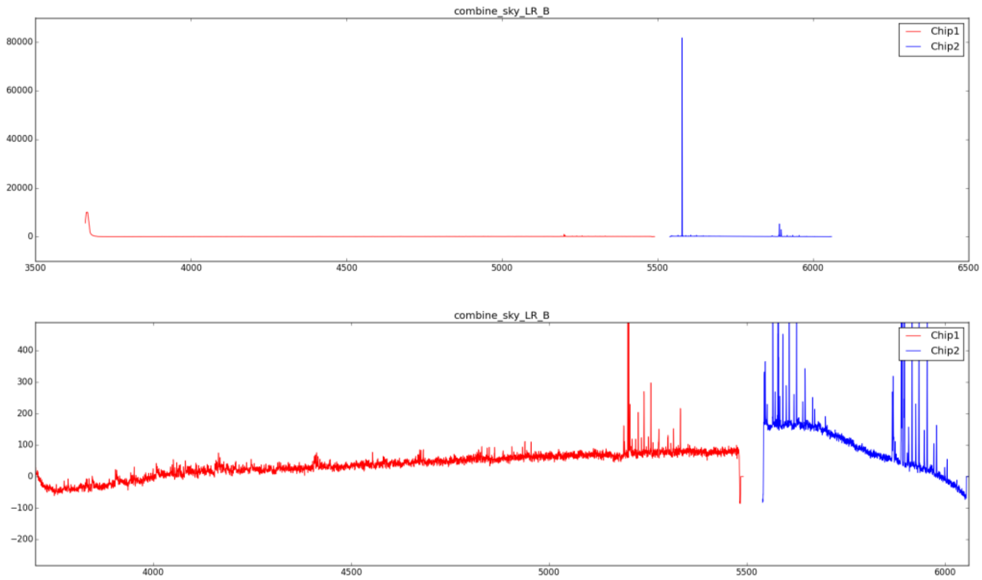

Figure 39 Combined sky spectra from the full 7 hours of STePS data for Low resolution in blue wavelength. The subtracted spectrum of an individual sky fibre does not differ significantly from the second panel of Figure 37.

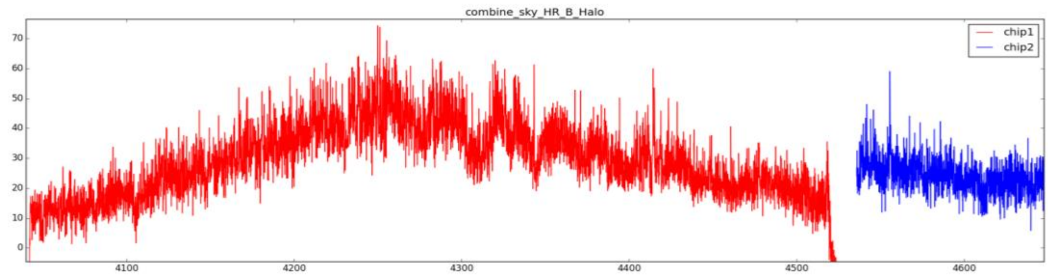

Figure 40 This spectrum is simulated sky from target spectrum from halo, High resolution in blue wavelength. The spectrum is 2 hours exposures template from Caffau et al.

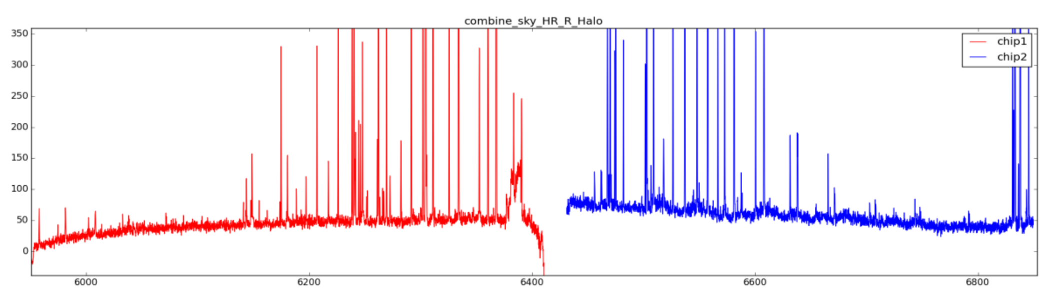

Figure 41 The spectrum is simulated sky from target spectrum from halo, High resolution in red wavelength.

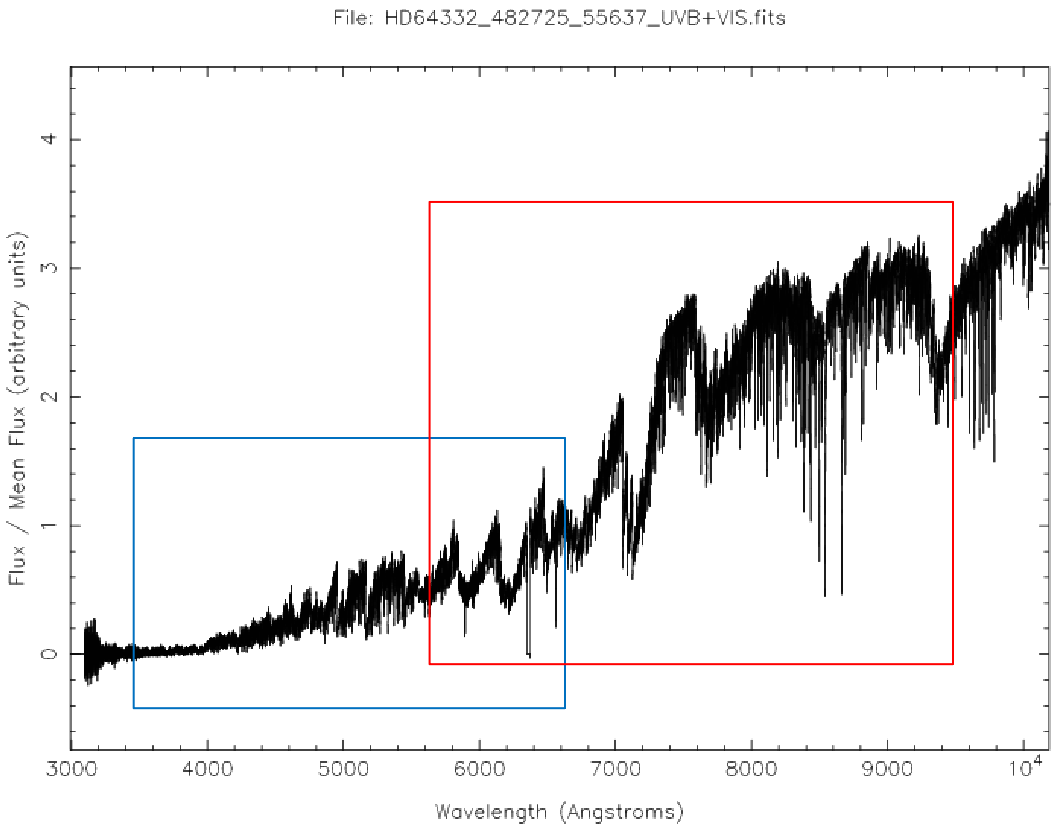

Figure 42 Template spectra showing galactic S star (variable), the blue box indicates the same range of blue wavelength from WEAVE and the red box indicates the range of red wavelength in Figure 43.

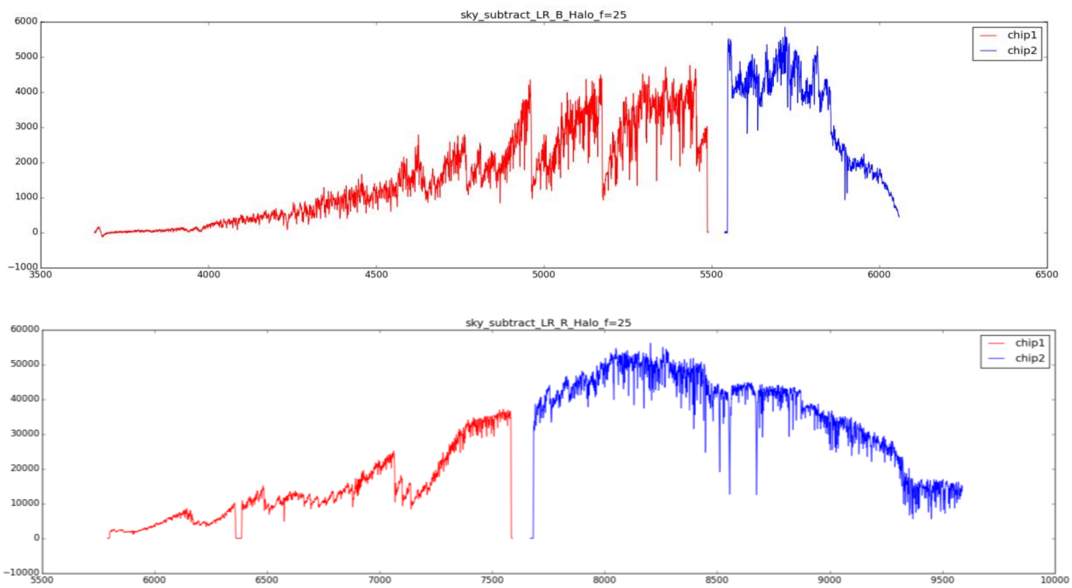

Figure 43 Regenerated spectra from WEAVESIM simulated 1 hour exposure image for the same star of V=15.17.

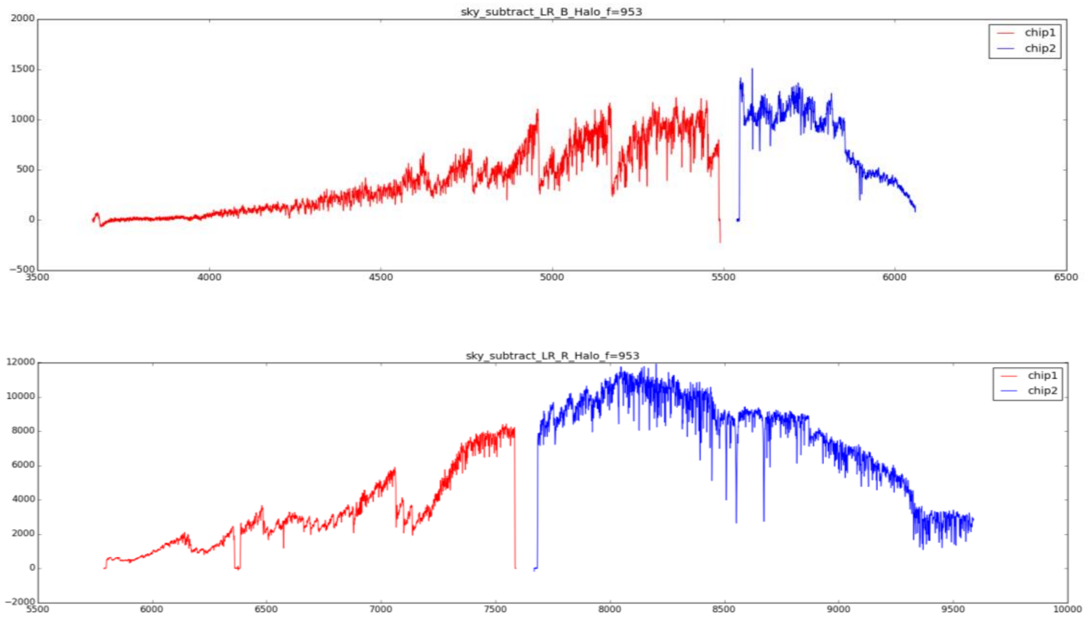

Figure 44 Regenerated spectra from WEAVESIM simulated 1 hour image for the same star of V=16.67. This spectra is from one of extreme fiber, f=953, and it shows fainter spectra on the whole than the spectra from f=25 in Figure 43.

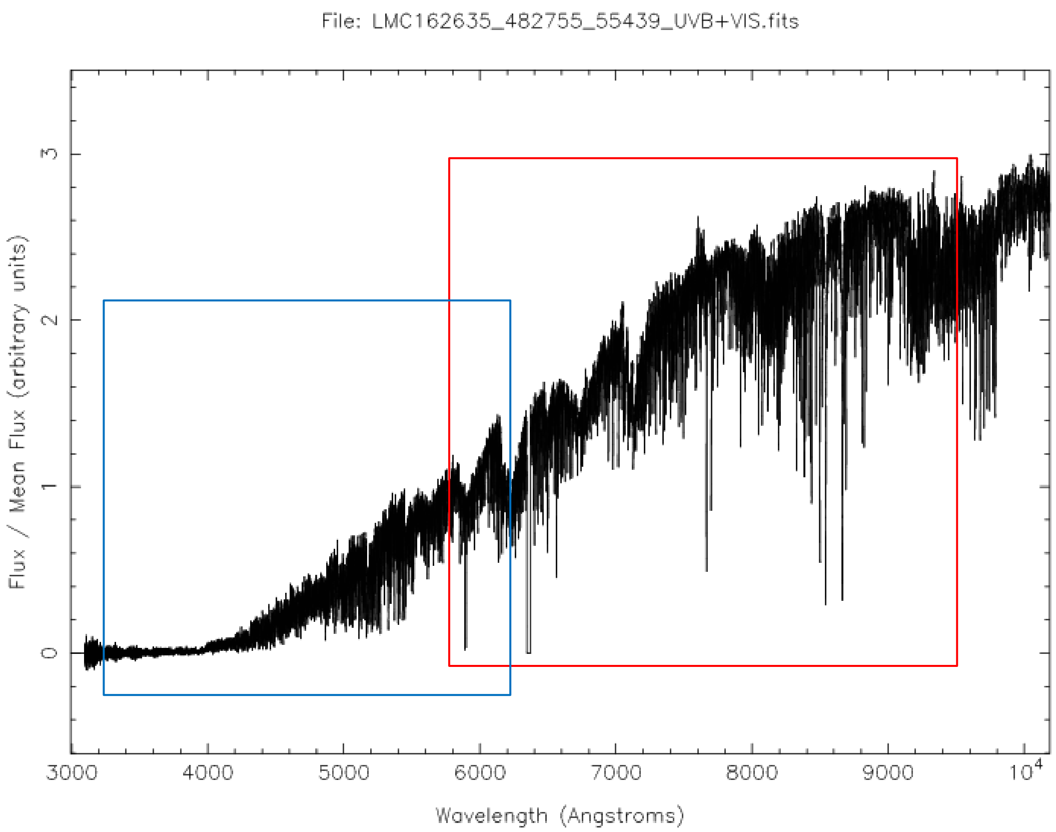

Figure 45 Template spectra of LMC162635_482755_55439_UVB+VIS (variable star) from XSL. The blue and red boxes indicate the same range of wavelength from WEAVE simulated image.

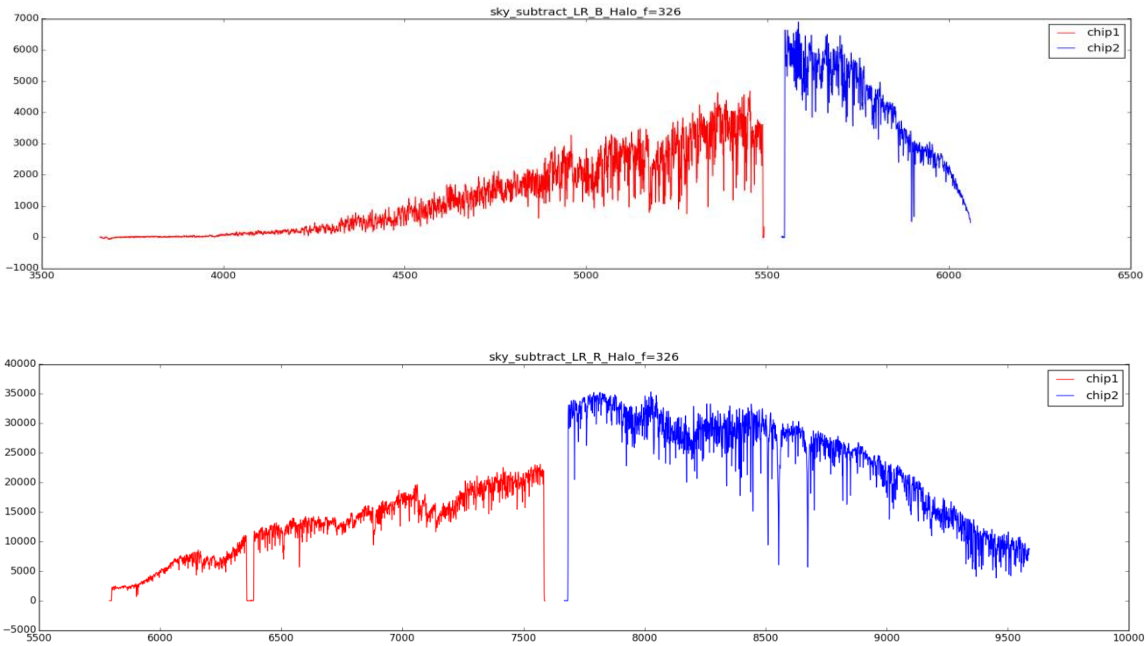

Figure 46 Recovered, sky-subtracted spectra from WEAVESIM. This is for the same star with V~15.13 for low resolution in blue (top) and red (bottom) band. The gap in the spectrum at 640nm is due to a dichroic element in XShooter.

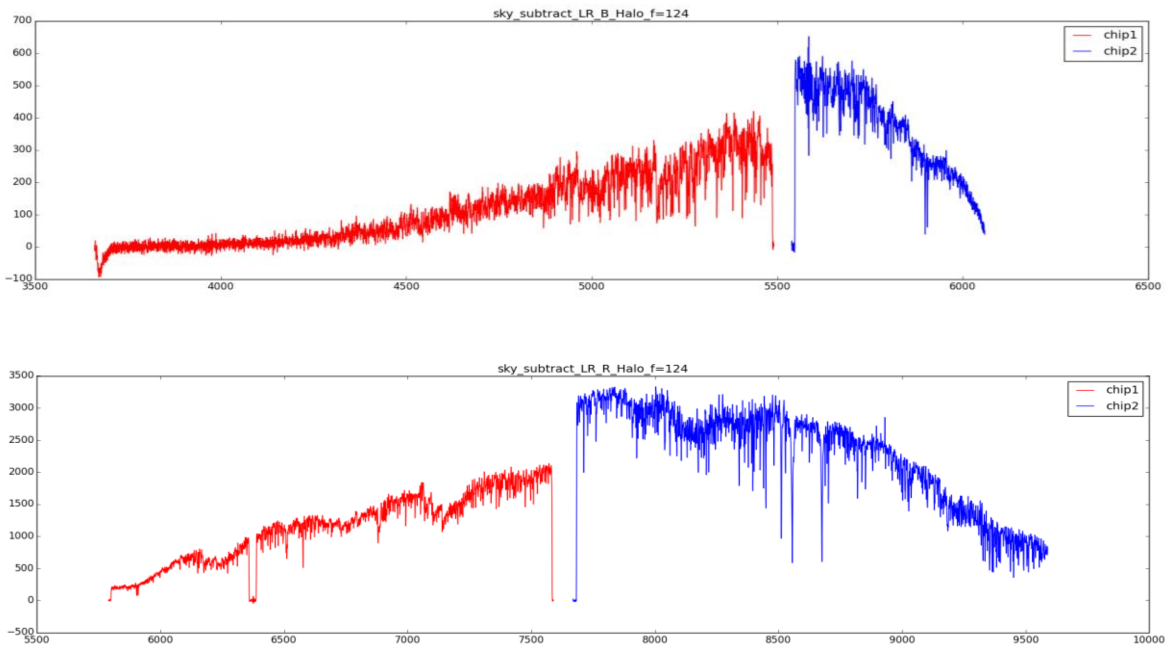

Figure 47 Recovered, sky-subtracted spectra from WEAVESIM. This is for an equivalent star, but different fiber number, f=124, with V~17.73 for low resolution in blue (top) and red (bottom) band.

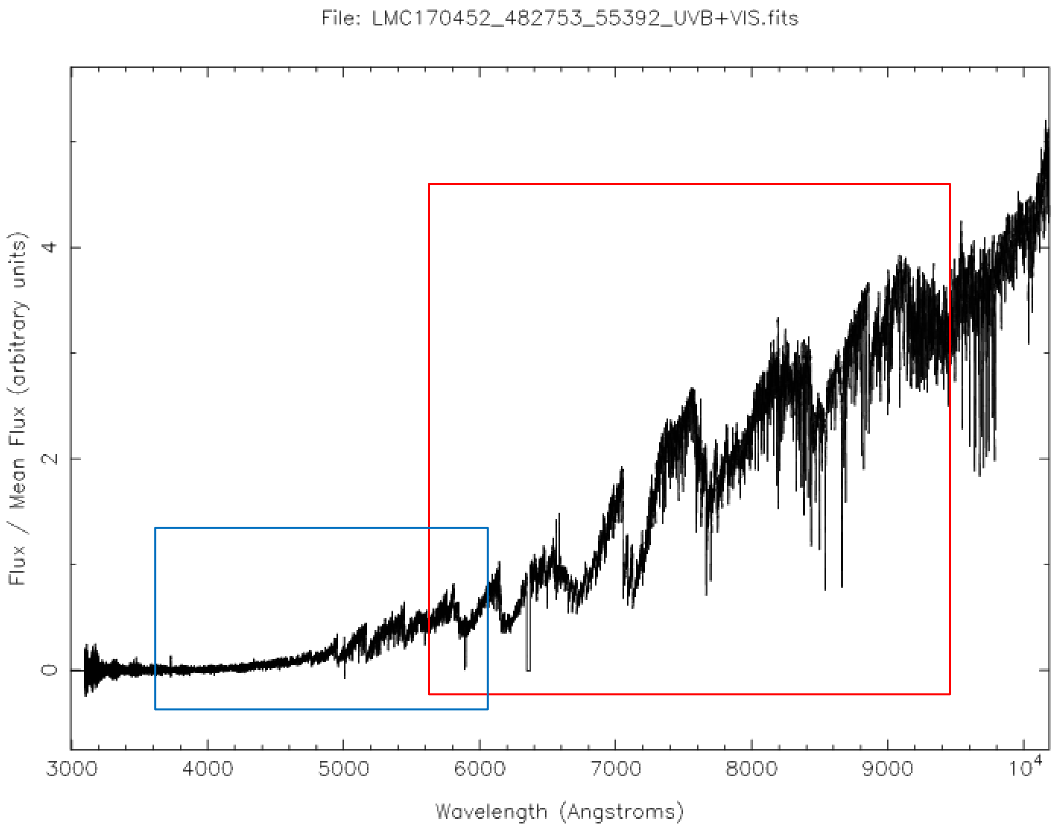

Figure 48 Template spectra of LMC170452_482753_55392_UVB+VIS (Red supergiant star) from XSL. The blue and red boxes indicate the same range of wavelength from WEAVE simulated image.

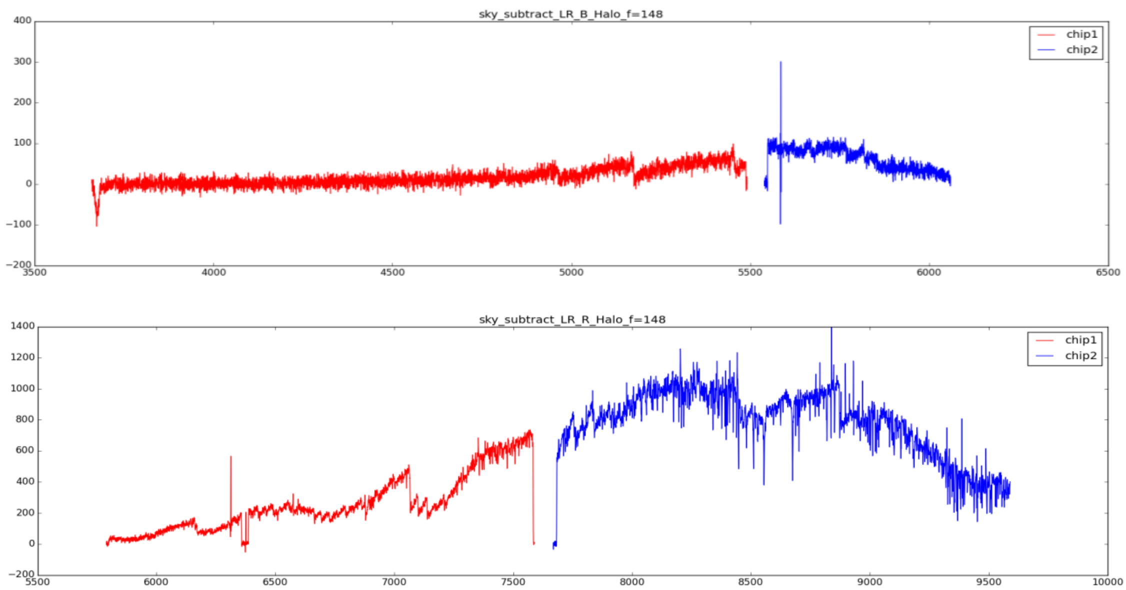

Figure 49 Regenerated spectra from WEAVESIM. This is from simulated halo field star (V~19.64) for low resolution in blue (top) and red (bottom) band. The template spectra is red supergiant star, therefore the regenerated spectra from the simulator in blue band shows unclear feature in the image.

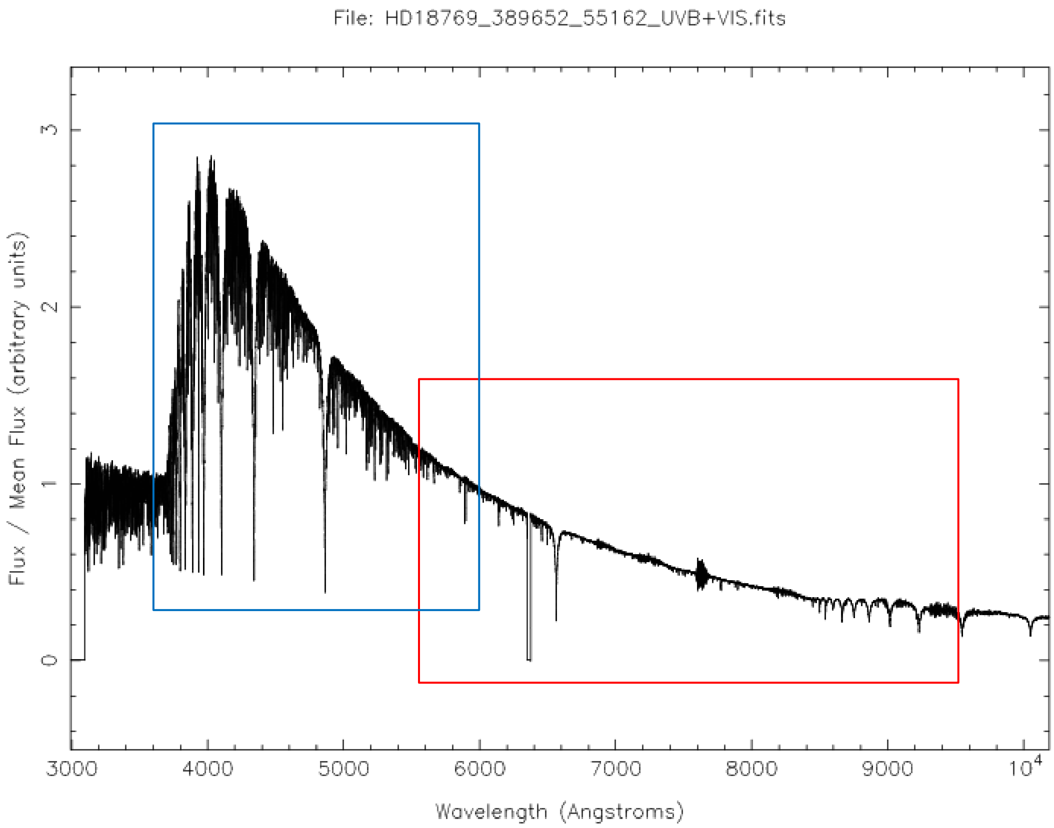

Figure 50 Template spectra of HD18769_389652_55162_UVB+VIS (variable star) from XSL. The blue and red boxes indicate the same range of wavelength from WEAVE simulated image.

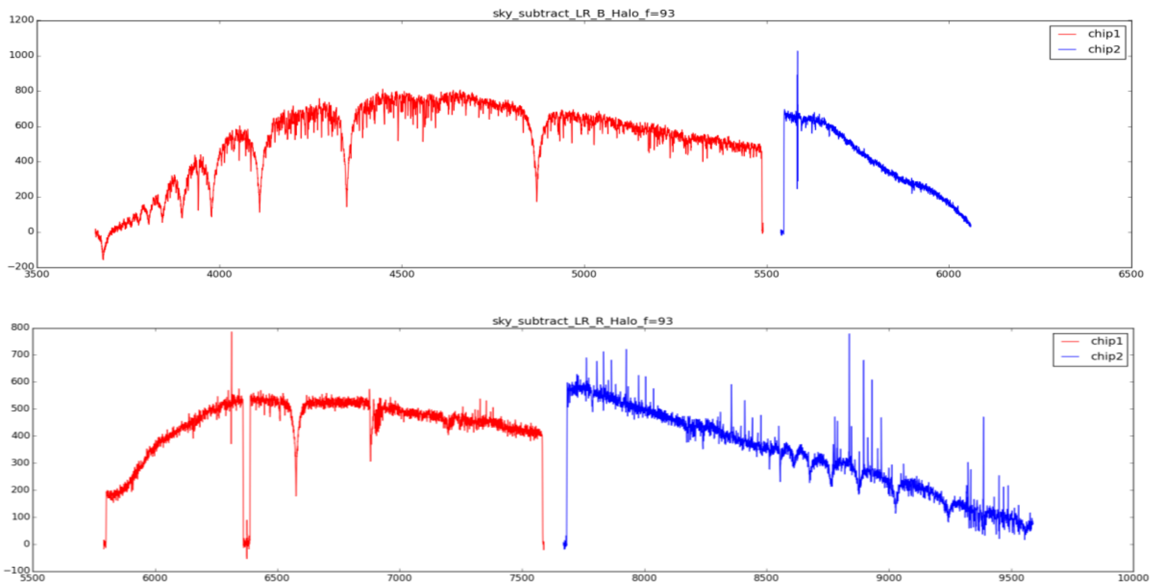

Figure 51 Regenerated spectra from WEAVESIM. This is from simulated halo field star (V~17.3) for low resolution in blue (top) and red (bottom) band. The lines from Hα to Hδ are shown in the spectra. The gap in the spectrum from bottom image is due to a dichroic element at 640nm in XShooter.

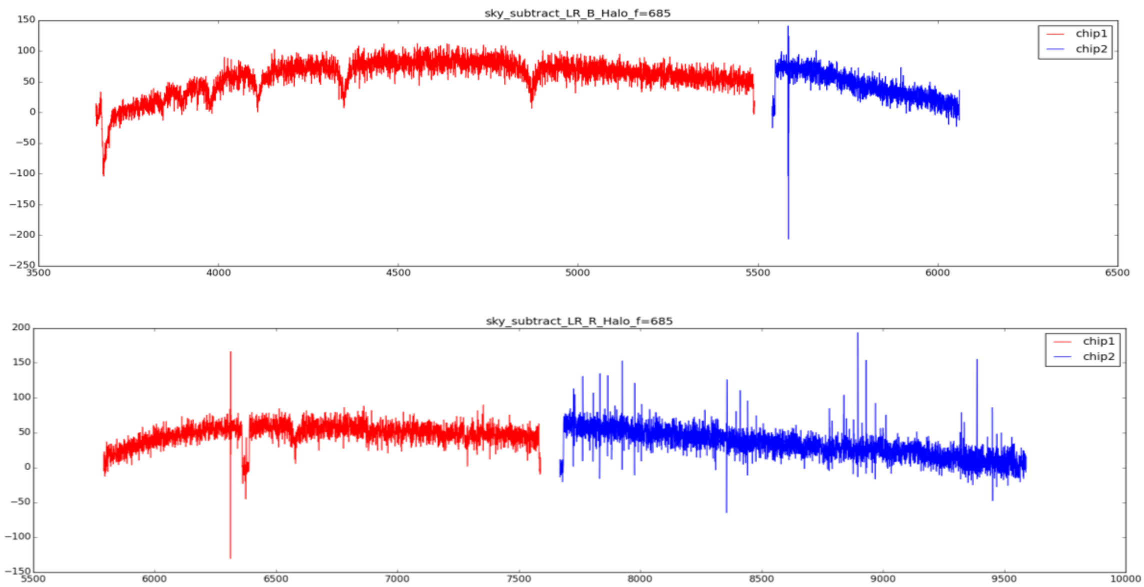

Figure 52 Regenerated spectra from WEAVESIM. This is from simulated halo field star (V~19.69) for low resolution in blue (top) and red (bottom) band. This is fainter spectra than the previous spectra in Figure 51, thus it has vague feature.

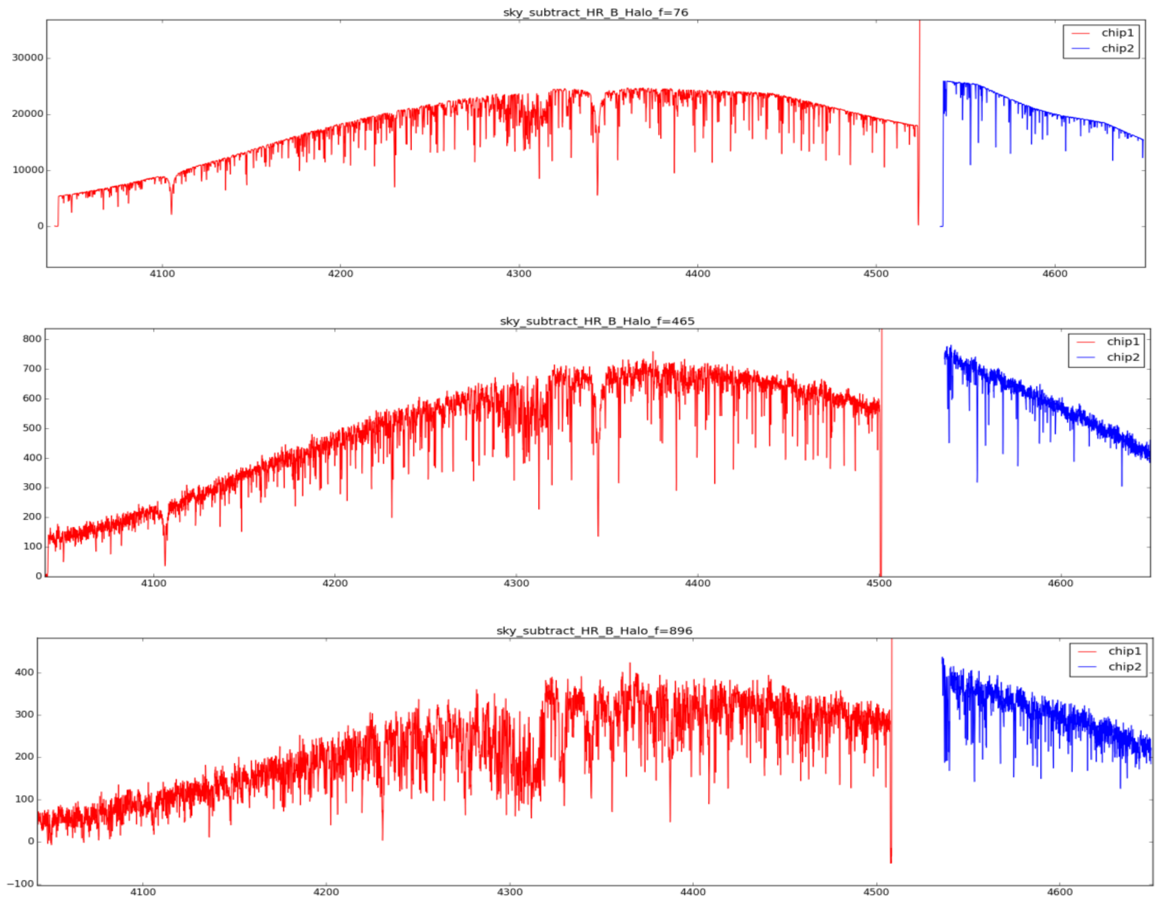

Figure 53 Regenerated final spectra in high resolution and blue band. From the top, the target star t5500g300a04m20r18_w370_700 for V~12.28, t5500g300a04m20r155_370_700 for V~14.02 and t4500g200a04m20r135_w370_700 for V~16.15

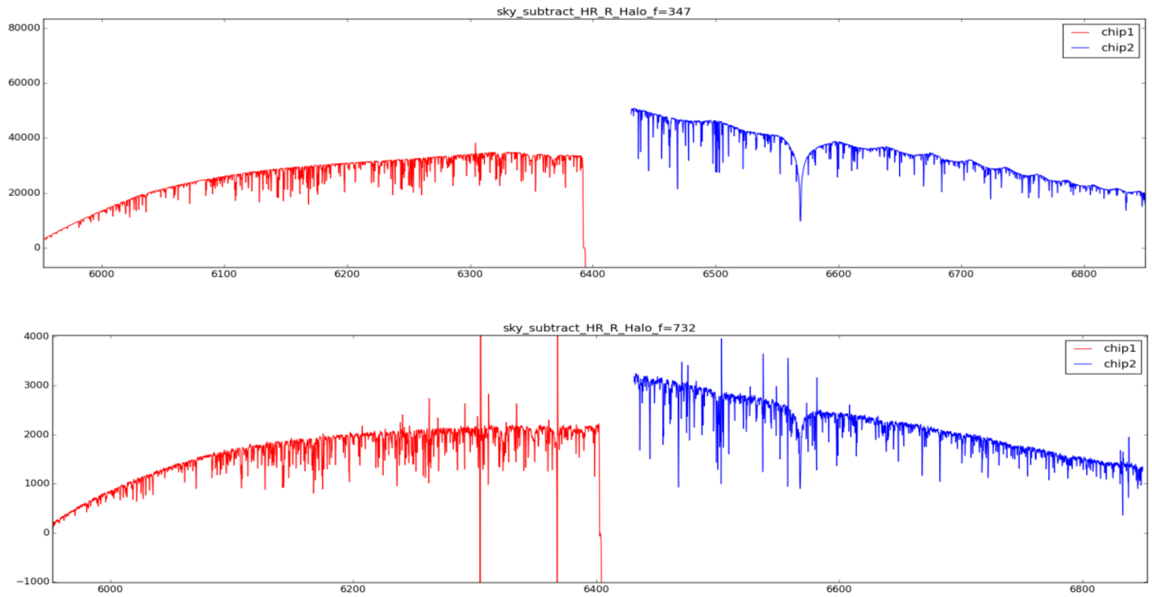

Figure 54 Regenerated final spectra in high resolution and red band. (Top) the target star t6500g300a00p05r155_w370_700 for V~12.433 and t4500g200a04m30r15_370_700 for V~11.990.

Chapter 5

CONCLUDING REMARK AND FUTURE WORKS

The WEAVE (WHT Extreme Aperture Velocity Explorer) data simulator has been developed for the WEAVE SPA (Science Processing and Archiving), this simulator can generate synthetic images to verify the scientific performance of WEAVE before the commissioning of the instrument. First, we derived PSFs and footprints of the fibre images from ray tracing in Zemax, and have developed the simulator to generate simulated spectral images using interpolation of the datasets from Zemax. Second, we performed a case study involving various stellar and galaxy spectra to regenerate synthetic spectra throughout the simulator and finally we showed the reliability of the simulator.

1) We use Zemax simulation by ray tracing for 480 data points, 9 different wavelengths and 5 configurations. The total datasets have 21600 points each.

2) We developed the simulator, WEAVESIM, to generate and extract synthetic spectra. From the datasets from Zemax used for this simulator; we made 3 dimensional arrays and calculated the interpolation of the PSFs with 20,000 wavelengths for a 21 x 21 pixel grid at each wavelength. Currently the simulator includes atmospheric effect such as seeing, scattering and transmission, cosmological parameter as Doppler effect and also fibre input. The further elements we need to revise or improve in the simulator describe in the future works.

3) In the case studies, we gathered the data from 1) STePS for low/high resolution in red and blue wavelengths 2) Low resolution simulated halo spectra in both arms, with stars from XSL/galaxies from [Kinney et al., 1996] and [Calzetti et al., 1994] 3) High resolution spectra in both arms, this is 2 hours exposure halo field using data from [Caffau et al., 2012]. The simulator generates representative spectra for each target realisation; therefore it can be applied for further testing to verify that the scientific objectives of WEAVE can be met.

The purpose of this study is not only for making simulated images for WEAVE, but also for validating the instrument data processing pipeline. This whole procedure is to verify and validate the WEAVE data flow including the data reduction and analysis pipelines before the delivery of the operational system. Thus we can provide the high signal to noise reference images to the pipeline team as fitting templates for the fibre positions and the PSF mapping.

The importance and benefits of developing the simulator are:

- Development of valid simulator before the spectrograph installed to the telescope
- Cost and time effective study without physical prototype of instrument design

- Early detection of possible errors or improper settings and improvements through continuous trade-off study
- Reliability test for design requirements
- Providing indicative test data for WEAVE community

For the next updates of the simulator, we have a plan to establish a direct link of the output with the fibre configuration tool, which is to allow users to generate representative outputs from simulated input datasets that will include all the positional and fibre-angle effects that will be relevant for the final data. It will include spatial vignetting functions at the telescope focal plane and also in the spectrograph system. As the figures are shown as below, WEAVESIM can generate valid synthetic spectrum. The regenerated throughput for high resolution mode from the simulator shows equivalent level of the total estimated throughput as a system performance of WEAVE.

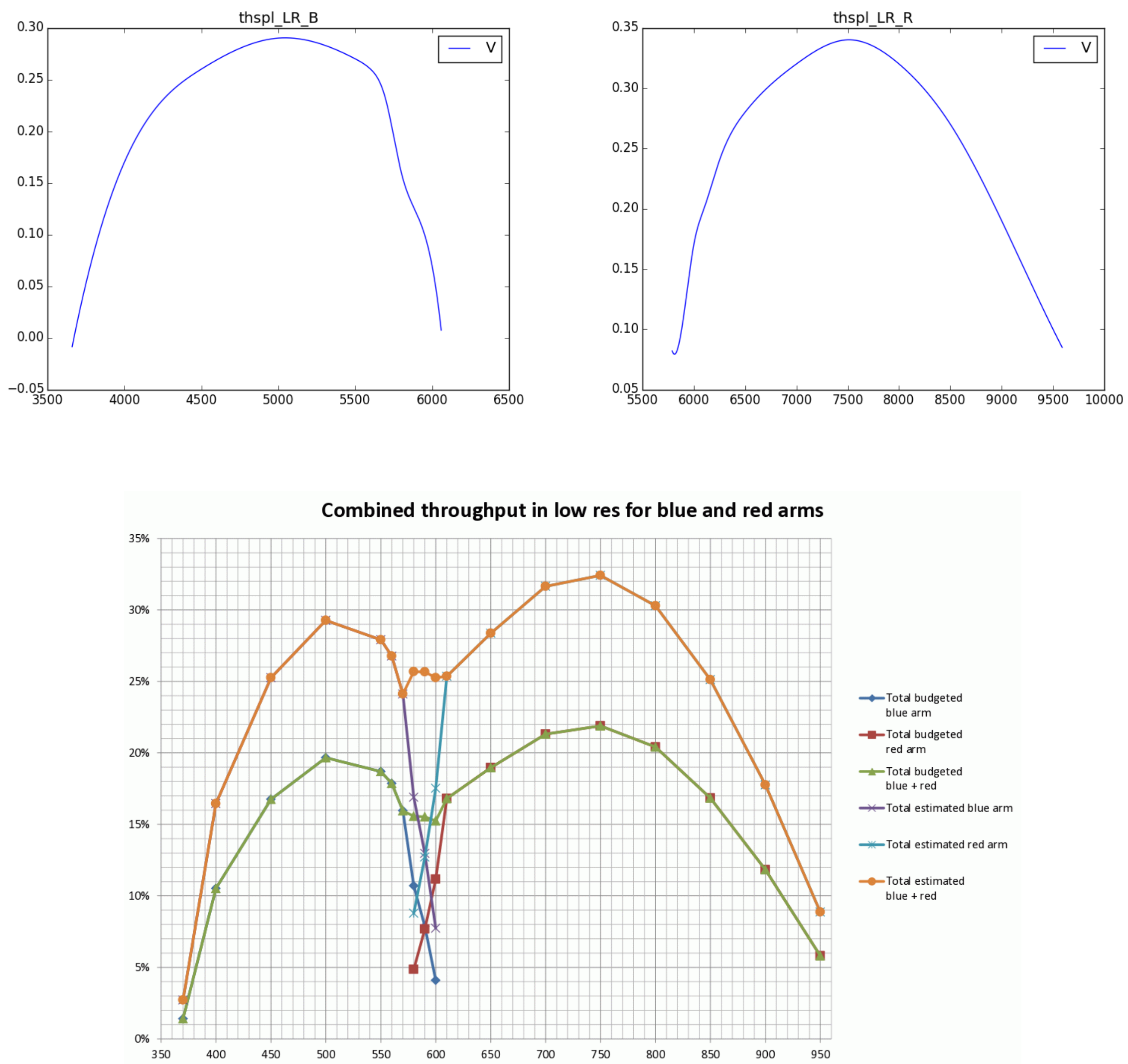

Figure 55 (Top pair) regenerated throughput from WEAVESIM in low resolution for blue and red arms. (bottom) Combined throughput in low resolution for both arms. The orange line shows total estimated throughput in blue and red band.

However there still remains scope for further study. As shown in Figure 56, the simple approach to extraction of the spectra introduces a ripple in the output spectrum. This was identified in the early phase of the study, and considerable effort was spent to figure out the cause. Given Zemax design file has been developed from the other team in the project, so we checked the constraints and environments for running the simulation first. The input data from Zemax were fully confirmed before applying into the Python. Finally we concluded that increasing the width of the extraction top-hat in the spatial direction from 5 pixels to 7 (or 9) effectively removes this effect, implying that the issue is with the extraction, not with the image itself. The true data pipeline will employ correct profile weighted extraction algorithms and will not be sensitive to this effect.

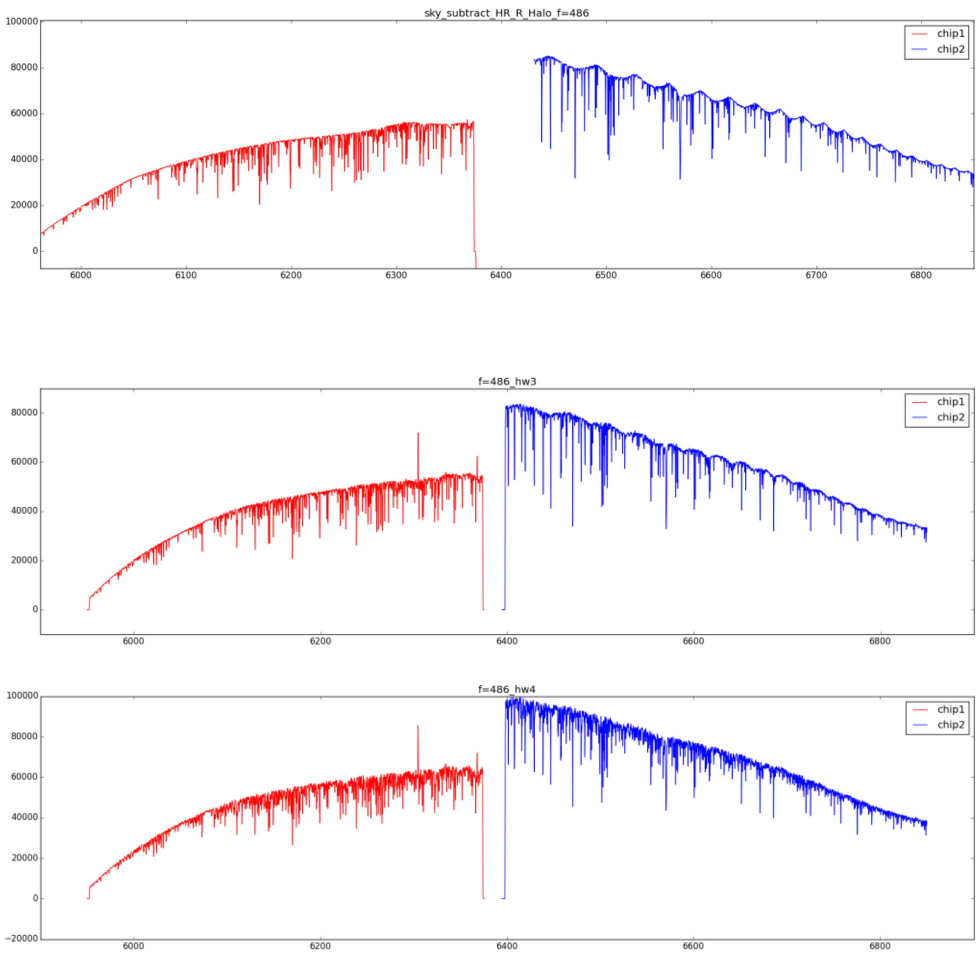

Figure 56 WEAVESIM generate ripple for some of synthetic spectra. Top image is the final spectrum of high resolution halo field in red wavelength, fibre number=486. Middle (sampling 7 pixels) and bottom (sampling 9pixels) spectra are from the same conditions of top image, except of increasing sampling of pixel for PSFs. The ripple decreased in sampling more pixels.

And the other remaining issue for the further study is over-subtraction of the sky spectra. We could identify the all positive residual from sky spectra we subtracted from template images. The one of possibilities is the input is contaminated from adjacent fibres, i. e. crosstalk problem or simply wrong scaling. For example the spectra in Figure 57 show better performance for this issue, this is divided by flat field. This procedure has been included in

CASU pipeline, extracting the spectra according to measured profile in the flat field image. It shows the spectra are much less sensitive to crosstalk. Another reason is that there spectra extract one data point per pixel in wavelength, rather than one data point per PSF location as the simulator works. So the signal-to-noise ratio is much higher than previous case study.

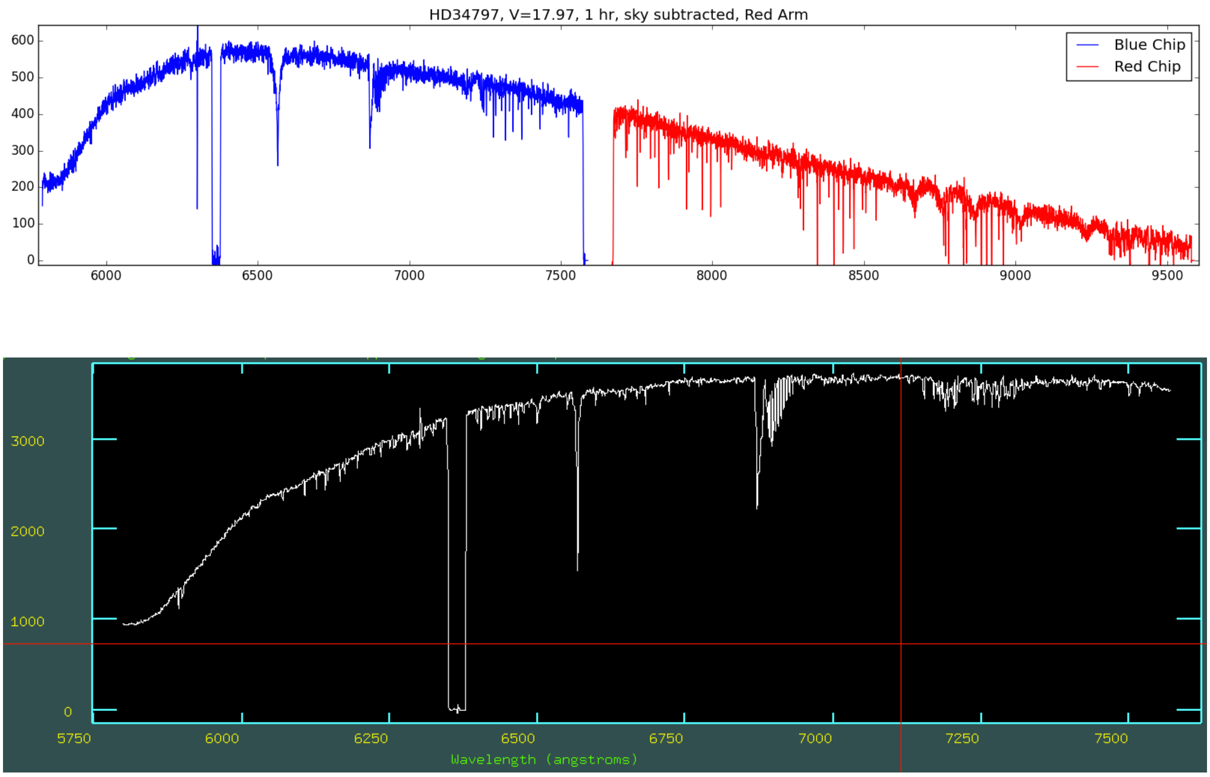

Figure 57 Top : Sky subtracted spectra of HD34797 for red arm. Bottom : normalized spectra by flat field. It shows high signal-to-noise and reduced positive residual.

Also we had planned to study crosstalk and scattering in the spectrograph, since WEAVE has high multiplex and it is therefore possible to overlap the image of adjacent fibres at some level. In the simulator, we calculate the PSF along the fibre and interpolate the values; they have to be overlapped by neighbor PSFs. Also the scattering problem has not yet been fully investigated. If the direction of the tip of fibre is changed, even though very small angle, it should be cause of stray lights and make ghost images on the detector as the stray light contribution from any one object to spectrum of any other is $<$ 0.5% as the system requirements. A further development, now that the simulator machinery is in place, would therefore now be to repeat the simulation with some tolerance variation of the chief ray angles in the input Zemax PSFs.

References

Agócs T., Abrams D. C., Lhomé E., Dee K., Dalton G. B., Middleton K., Bonifacio P., Aguerri J. A. L., Trager S. C., 2014, SPIE, Ground-based and Airborne Instrumentation for Astronomy V, Vol. 9147, 73

Allard F., Homeier D., Freytag B., 2011, The Astronomical Society of Pasific Conference Series, Vol. 448

Balcells M., Benn C. R., Carter D., Dalton G. B., Trager S. C., Feltzing S., Verheijen M. A. W., Jarvis M., Percival W., Abrams D. C., Agocs T., Brown A. G. A., Cano D., Evans C., Helmi A., Lewis I. J., McLure R., Peletier R. F., Pérez-Fournon I., Sharples R. M., Tosh I. A. J., Trujillo I., Walton N., Westfall K. B., 2010, in Society of Photo-Optical Instrumentation Engineers (SPIE) Conference Series, Instrumentation and Methods for Astrophysics, Vol. 7735, 57

Berk A., Bernstein L. S., Anderson G. P., Acharya P. K., Robertson D. C., Chetwynd J. H., Alder-Golden S. M., 1998, Remote Sensing of Environment, 65:367-375

Burgh E. B., Bershady M. A., Westfall K. B., Nordsieck K. H., 2007, Astronomical Society of the Pacific, Vol. 119, 1069

Caffau E., Koch A., Sbordone L., Sartoretti P., Hansen C. J., Royer F., Leclerc N., Bonifacio P., Christlieb N., Ludwig H. -G., Grebel E. K., De Jong R. S., Chiappini C., Walcher J., Mignot S., Feltzing S., Cohen M., Minchev I., Helmi A., Piffl T., depagne E., Schnurr O., 2013, Astronomische Nachrichten, AN334, No. 3, 197-216

Calzetti D., Kinney A. L., 1994, The Astonomical Journal, 429:582-601

Chemla F., Dalton G. B., Guinouard I., Pragt J., Sawyer E., Spanò P., Tosh I. A., Andersen M. I., Navarro R., Hammer F., Kaper L., 2010, SPIE, Ground-based and Airborne Instrumentation for Astronomy Ⅲ, Vol. 7735, 5

Chen Y- P., Trager S. C., Peletier R. F., Lançon A., Vazdekis A., Prugniel Ph, Silva D. R., Gonneau A., 2014, Astronomy and Astrophysics, 565, A117

Coelho P., 2014, MNRAS, 440, 1027-1043

Coelho P., Bruzual G., Charlot S., Weiss A., Barbuy B., Ferguson J. W., 2007, MNRAS, 382, 498-514

Craig N., Abbott M., Finley D., Jessop H., Howell S. B., Mathioudakis M., Sommers J., Vallerga J. V., Malina R. F., 1997, The Astonomical Journal Supplement Series, 113:131-193

Dalton G. B., Trager S. C., Abrams D. C., Carter D., Bonifacio P., Aguerri J. A. L., MacIntosh M., Evans C., Lewis I. J., Navarro R., Agocs T., Dee K., Rousset S., Tosh I., Middleton K., Pragt J., Terrett D., Brock M., Benn C., Verheijen M., Cano D., Bevil C., Steele I., Mottram C., Bates S., Gribbin F., Rey J., Rodriguez L. F., Delgado J. M., Guinouard I., Walton N., Irwin M., Jagourel P., Stuik R., Gerlofsma G., Roelfsma R., Skillen I., Ridings A., Balcells

M., Daban J- B., Gouvret C., Venema L., Girard P., 2012, SPIE, Ground-based and Airborne Instrumentation for Astronomy IV, Vol 8446, 23

Dalton G. B., Trager S. C., Abrams D. C., Carter D., Bonifacio P., Aguerri J. A. L., Middleton K., Benn C., Dee K., Sayède F., Lewis I. J., Pragt J.,Pico S., Walton N., Rey J., Prieto G. A., Peňate J., Lhome E., Agócs T., Alonso J., Terrett D., Brock M., Gilbert J., Ridings A., Guinouard I., Verheijin M., Tosh I. A., Rogers K., Steele I., Stuik R., Tromp N., Jasko A., Hragt J., Lesman D., Mottram C., Bates S., Gribbin F., Rodriguez L. F., Delgado J. M., Martin C., Cano D., Navarro R., Irwin M., Lewis J., Solares E. G., O'Mahony N., Bianco A., Zurita C., Ter Horst R., Molinari E., Lodi M., Guerra J., Vallenari A., Baruffolo A., 2014, SPIE, Instrumentation and Methods for Astrophysics, Vol. 9147, 11

Fiorino S. T., Randall R. M., Via M. F., Burley J. L., 2013, Journal of Applied Meteorology and Climatology, Vol. 53, 136

Goodwin M., Smedley S., Barnes S., Farrell T., Barden S., 2010, SPIE, Ground-based and Airborne Instrumentation for Astronomy Ⅲ, Vol. 7735, 77357U

Iovino A., Pozzetti L., Mercurio A, 2014, WEAVE-Stellar Populations at Intermediate Redshifts survey SP®Itz-StePs-StAIRS

Irwin M., Lewis J., Walton N., Gonzalez-Solares E., 2015, WEAVE-CPS-003, WEAVE Core Processing System Software Development Plan

Jin Z., Charlock T, P., Rutledge K., Stamnes K., Wang Y., 2006, Applied Optics, Vol. 45, No. 28

Kinney A. L., Calzetti D., Bohlin R., McQuade K., Storchi-Bergmann T., Schmitt H. R., 1996, The Astronomical Journal, 467:38-60

Lewis I. J., Cannon R. D., Taylor K., Glazebrook K., Bailey J. A., Baldry I. K., Barton J. R., Bridges T. J., Dalton G. B., Farrell T. J., Gray P. M., Lankshear A., McCowage C., Parry I. R., Sharples R. M., Shortridge K., Smith G. A., Stevenson J., Straede J. O., Waller L. G., Whittard J. D., Wilcos. J. K., Willis K. C., 2002, Monthly Notices of the Royal Astronomical Society, 333, 279-298

Math Works, The value of model-based design, www.mathworks.com

Meyer M., Edwards S., Hinkle K. H., Strom S., 1998, The Astrophysical Society, 508:397-409

Navarro R., Chemla F., Bonifacio P., Flores H., Guinouard I., Huet J- M., Puech M., Royer F., Pragt J. H., Wulterkens G., Sawyer E. C., Caldwell M. E., Tosh I. A. J., Whalley M. S., Woodhouse G. F. W., Spanò P., Di Marcantonio P. Andersen M. I., Dalton G. B., Kaper L., Hammer F., 2010, SPIE, Ground-based Airborne Instrumentation for Astronomy Ⅲ, Vol. 7735, 2

Noll S., Kausch W., Barden M., Jones A. M., Szyszka C., Kimeswenger S., 2013, VLT-

MAN-ESO-19550-5339, The Cerro Paranal Advanced Sky Model

Noll S., Kausch W., Barden M., Jones A. M., Szyszka C., Kimeswenger S., Vinther J., 2012, A&A, 543, A92

Palacios A., Gebran M., Josselin E., Martins F., Plez B., Belmas M., Lèbre A., 2010, A&A, 516, A13

Pickles A. J., 1998, Publications of the Astronomical Society of the Pacific, 110:863-878

Prugniel Ph., Soubrian C., 2001, A&A, 369, 1048-1057

Prugniel Ph., Soubrian C., 2004, ArXiv e-prints, 0409214

Rogers K., Stuik R., Steele I. A., Pragt J., Middleton K. F., Bates S., Kragt J., Tromp N., Lesman D., Lhomé E., Dalton G. B., Trager S. C., Navarro R., Abrams D. C., Tosh I. A., Jasko A., Martin C., O'Mahony N., Pico S., Infantes D. C., Bianco A., Delgado J., Rodriguez L., F., 2014, SPIE, Ground-based and Airborne Instrumentation for Astronomy V, Vol. 91476H

Rothman L. S., Gordon I. E., Babikov Y., Barbe A., Benner D. C., Bernath P. F., Birk M., Bizzocchi L., Boudon V., Brown L. R., Campargue A., Chance K., Cohen E. A., Coudert L. H., Devi V. M., Drouin B. J., Fayt A., Flaud J. -M., Gamache R. R., Harrison J. J., Hartmann J. -M., Hill C., Hodges J. T., Jacquemart D., Jolly A., Lamouroux J., Le Roy R. J., Li G., Long D. A., Lyulin O. M., Mackie C. J., Massie S. T., Milhailenko S., Műller H. S. P., Naumenko O. V., Nikitin A. V., Orphal J., Perevalov V., Perrin A., Polovtseva E. R., Richard C., Smith M. A. H., Starikova E., Sung K., Tashkun S., Tennyson J., Toon G. C. Tyuterev Vl. G., Wagner G., 2013, Journal of Quantitative Spectroscopy & Radiative Transfer, 130, 4-50

Smith D., Jarvis M., Röttgering H., Simpson C. and the WEAVE-LOFAR science team, The WEAVE-LOFAR Survey, 2015

Trager S. C. and Science Teams, 2015, WEAVE-SCI-005, The WEAVE Surveys: Strategy and Planning

Trager S. C. and Science Teams, WEAVE-SCI-002, The WEAVE Science Case, 2015

Verheijin M. A. W., Oosterloo T. A., Van Capellen W. A., Bakker L., Ivashina M. V., Van der Hulst J. M., 2008, American Institute of Physics (AIP) Conference Proceedings, 1035, 265

Walcher C. J., Coelho P., Gallazzi A., Charlot S., 2009, MNRAS, 398, L44-L48

Walton N. A., Irwin M., Lewis J. R., Gonzalez-Solares E., Dalton G. B., Trager S. C., Aguerri J. A. L., Prieto C. A., Benn C. R., Abrams D. C., Pico S., Middleton K., Lodi M., Bonifacio P., 2014, SPIE, Software and Cyberinfrastructure for Astronomy Ⅲ, Vol. 91520R

Walton N., Irwin M., Gonzalez-Solares E., Lewis J., 2015, WEAVE-CPS-001, WEAVE Core Processing System Requirements and Technical Description

Walton N., Irwin M., Gonzalez-Solares E., Lewis J., Lodi M., Zurita C., 2015, WEAVE-SPA-001, WEAVE Science Processing and Analysis System Description and Overview

Worthey G., Ottaviani D. L., 1997, The Astronomical Journal Supplement Series, 111:377-386

Zemax User's Manual, Radiant ZEMAX LLC, 2011